

A beginner's guide to low-coverage whole genome sequencing for population genomics

Runyang Nicolas Lou^{1*}, Arne Jacobs^{1,2}, Aryn Wilder³, Nina O. Therkildsen^{1*}

¹Department of Natural Resources and the Environment, Cornell University, Ithaca, NY 14853, USA

²Current address: Institute of Biodiversity, Animal Health and Comparative Medicine, University of Glasgow, Glasgow, G12 8QQ, UK

³San Diego Zoo Wildlife Alliance, Escondido, CA 92027, USA

*Corresponding authors: RNL (rl683@cornell.edu), NOT (nt246@cornell.edu)

Abstract

Low-coverage whole genome sequencing (lcWGS) has emerged as a powerful and cost-effective approach for population genomic studies in both model and non-model species. However, with read depths too low to confidently call individual genotypes, lcWGS requires specialized analysis tools that explicitly account for genotype uncertainty. A growing number of such tools have become available, but it can be difficult to get an overview of what types of analyses can be performed reliably with lcWGS data, and how the distribution of sequencing effort between the number of samples analyzed and per-sample sequencing depths affects inference accuracy. In this introductory guide to lcWGS, we first illustrate how the per-sample cost for lcWGS is now comparable to RAD-seq and Pool-seq in many systems. We then provide an overview of software packages that explicitly account for genotype uncertainty in different types of population genomic inference. Next, we use both simulated and empirical data to assess the accuracy of allele frequency and genetic diversity estimation, detection of population structure, and selection scans under different sequencing strategies. Our results show that spreading a given amount of sequencing effort across more samples with lower depth per sample consistently improves the accuracy of most types of inference, with a few notable exceptions. Finally, we assess the potential for using imputation to bolster inference from lcWGS data in non-model species, and discuss current limitations and future perspectives for lcWGS-based population genomics research. With this overview, we hope to make lcWGS more approachable and stimulate its broader adoption.

Keywords: genotype likelihoods, bioinformatics, allele frequencies, population structure, selection scan, genotype imputation

42 1. Introduction

43

44 Despite massive reductions in the cost of DNA sequencing over the past decades, researchers
45 remain faced with decisions about how to distribute sequencing effort along three dimensions:
46 1) how much of the genome to sequence (breadth of coverage), 2) how deeply to sequence
47 each sample (depth of coverage), and 3) the total number of samples to sequence. Until
48 recently, reduced-representation sequencing (e.g. RAD-seq), through which a small random
49 portion of the genome can be sequenced deeply in many individuals to allow for simultaneous
50 variant discovery and high-confidence genotyping, has been the most popular approach for
51 population genomics of non-model organisms (Andrews, Good, Miller, Luikart, & Hohenlohe,
52 2016; Davey et al., 2011; McKinney, Larson, Seeb, & Seeb, 2017). While this approach
53 undoubtedly has led to a breakthrough in our ability to examine genome-wide patterns of
54 variation, an important limitation is that large stretches of the genome between markers remain
55 unsampled (Figure 1A). Accordingly, RAD-seq data may miss signatures of selection and
56 adaptive divergence that are highly localized in the genome (Lowry et al., 2017; Tiffin & Ross-
57 Ibarra, 2014).

58

59 In a growing number of cases, whole genome sequencing has identified striking peaks of
60 differentiation or strong associations with phenotypes that went completely undetected with
61 RAD-seq data [see e.g. 1) Aguillon, Walsh, & Lovette, 2020 vs. Aguillon, Campagna, Harrison,
62 & Lovette, 2018; 2) Campagna et al., 2017 vs. Campagna, Gronau, Silveira, Siepel, & Lovette,
63 2015; 3) Clucas, Lou, Therkildsen, & Kovach, 2019 vs. Clucas et al., 2019; and 4) Szarmach,
64 Brelsford, Witt, & Toews, 2021], suggesting that full genome coverage often is needed to
65 understand mechanisms of adaptation. However, whole genome sequencing at sufficient depths
66 to confidently call individual genotypes is still prohibitively expensive on a population scale for
67 many projects. A popular cost-effective alternative is to sequence pools of individuals (Pool-seq;
68 Schlötterer, Tobler, Kofler, & Nolte, 2014; Figure 1B). When the number of individuals pooled
69 and sequencing depth are sufficient, Pool-seq is a powerful approach for obtaining reliable
70 estimates of population-level parameters (Futschik & Schlötterer, 2010; Zhu, Bergland,
71 González, & Petrov, 2012). However, all information about individuals is lost, making it difficult
72 to control for uneven contribution to the pool and precluding individual-level analyses as well as
73 detection of cryptic substructure among sampled individuals (Anderson, Skaug, & Barshis,
74 2014; Fuentes-Pardo & Ruzzante, 2017).

75

76 Low-coverage whole genome sequencing (lcWGS) is emerging as a cost-effective alternative
77 that allows population-scale screening of the entire genome while retaining individual
78 information for - in many cases - a comparable cost to RAD-seq and Pool-seq. The underlying
79 strategy is to maximize the information content in the sequence data by spreading it across the
80 entire genomes of many separately barcoded individuals (Figure 1C). This way, we sacrifice
81 depth of coverage (repeated sequencing of the same locus in the same individual), and
82 therefore confidence in individual genotypes, in return for much greater breadth of coverage and
83 potentially also larger sample sizes.

84

85 At low depth of coverage, individual genotypes cannot reliably be inferred (Nielsen,
86 Korneliussen, Albrechtsen, Li, & Wang, 2012; Nielsen, Paul, Albrechtsen, & Song, 2011).
87 However, for most population-level questions, it is not the specific genotype of any particular
88 individual that matters, but rather the overall population characteristics (e.g. allele frequencies,
89 linkage disequilibrium (LD) patterns, etc). Similarly, for questions about genetic relationships
90 between individuals, it is not the genotype at any particular single nucleotide polymorphism
91 (SNP) that matters, but rather patterns of variation across SNPs genome-wide. Accordingly,
92 probabilistic analysis frameworks that account for uncertainty about the true genotype (instead
93 of assuming that any one genotype is correct) can integrate over the uncertainty about
94 individual genotypes for population-level inference of variation at particular SNPs (e.g. allele
95 frequencies, population differentiation), and integrate over the uncertainty about an individual's
96 genotype at each particular SNP to make inference about that individual's overall genetic
97 signature (e.g. level of inbreeding, admixture proportions; Buerkle & Gompert, 2013; Nielsen et
98 al., 2012, 2011).

99
100 Simulation studies have demonstrated that when sequencing data are analyzed within this type
101 of probabilistic statistical framework that accounts for genotype uncertainty, sampling many
102 individuals each at low read depth actually provides more accurate estimates of many
103 population parameters than higher read depth for fewer individuals (Buerkle & Gompert, 2013;
104 Fumagalli, 2013; Nevado, Ramos-Onsins, & Perez-Enciso, 2014). In fact, these studies have
105 suggested that spreading sequencing depth to 1–2 reads per locus and individual (1–2x
106 coverage or less) - and increasing sample sizes accordingly - maximizes the information gained
107 about a population. Many recent empirical studies have demonstrated the power of this
108 approach (examples are listed in Table S1). Some of the first applications included identification
109 of genomic regions repeatedly associated with marine-freshwater adaptation in stickleback
110 (Jones et al., 2012), adaptation to an Arctic lifestyle in polar bears (Liu et al., 2014), and
111 divergence among killer whale ecotypes (Foote et al., 2016). More recently, lcWGS was used
112 e.g. to identify genes involved in rapid adaptation to fisheries-induced size selection in
113 experimental populations of Atlantic silversides (Therkildsen et al., 2019), map hybrid
114 incompatibility genes in swordtail fish (Powell et al., 2020), scan for soft sweeps in response to
115 white-nose syndrome in bats (Gignoux-Wolfsohn et al., 2021), build ultra-dense crossover maps
116 in *Arabidopsis* (Rowan et al., 2019), and assess admixture patterns and elevated differentiation
117 across massive linkage blocks along environmental gradients in several non-model organisms
118 (Clucas et al., 2019; Mérot et al., 2021; Wilder, Palumbi, Conover, & Therkildsen, 2020).

119
120 Yet, despite the clear promise, adopting a lcWGS approach can seem daunting because
121 working with genomic data in a probabilistic framework requires both a shift in the way we think
122 about our data and a different toolbox that incorporates genotype uncertainty in downstream
123 analysis. In recent years, there has been a proliferation of programs that can explicitly account
124 for genotype uncertainty in population genomic inference. But for newcomers, it can be difficult
125 to get an overview of what types of analyses can reliably be performed with this data type and
126 what experimental designs will provide the most robust results for a particular system and
127 question, e.g. how to best divide a given sequencing effort between the number of samples vs.
128 the depth of sequencing per sample.

129
130
131
132
133
134
135
136
137
138
139
140
141
142
143
144
145
146
147
148
149
150
151
152
153
154
155
156
157
158
159
160
161
162
163
164
165
166
167
168
169

The goal of this paper is to provide a practical “field guide” for researchers considering a lcWGS approach. We first illustrate that lcWGS is now a feasible option for many research projects by comparing the current costs and requirements of lcWGS to alternative sequencing strategies (Section 2). Next, we introduce the basic statistical framework used to account for genotype uncertainty inherent to lcWGS data, and provide an overview of current analytical tools built under a probabilistic framework to help readers identify software that can robustly perform common types of population genomics inference with lcWGS data (Section 3). To guide experimental design, we then use both genetic simulations (Section 4) and down-sampling of empirical data (Section 5) to assess the accuracy of population genomic inference under different sequencing strategies. We evaluate trade-offs between sample size and depth of coverage, compare the power of lcWGS to RAD-seq and Pool-seq, and explore the potential of genotype imputation for bolstering inference with lcWGS data. Finally, in Sections 6 and 7, we review challenges and limitations associated with lcWGS data and discuss future perspectives. With this practitioner-centered overview, we hope to make lcWGS more accessible to a wider group of researchers and stimulate broader adoption of this powerful approach, while inspiring future development of population genomic inference methods for lcWGS data.

2. Feasibility: What does lcWGS cost and what resources are required?

2.1 Current sequencing costs

It is a widespread assumption that whole genome sequencing approaches are still too expensive for researchers working on modest budgets. Yet, due to spectacular drops in sequencing costs over the past decades (the cost per Mb of sequencing is today >600,000 times cheaper than in 2000; Wetterstrand, 2021), lcWGS can now - in many cases - be performed at similar per-sample costs as reduced-representation techniques. Table 1 provides estimates of the total per-sample cost for both library preparation and sequencing (based on May 2021 pricing) for organisms of different genome sizes. The cost of lcWGS inevitably scales with genome size (because more sequence data are needed to provide a target coverage level of a large vs. a small genome), and this approach therefore may remain impractical for organisms with extremely large genome sizes. However, even for organisms with sizeable genomes around 1 Gb (e.g. many birds, fish, invertebrates, and plants), the per-sample cost with 1-2x sequencing coverage (20-35 USD) is now on par with the 30 USD recently reported for genotyping 20,000 variable RAD-seq loci, the 15 USD for a custom sequence capture approach for 500 - 10,000 loci (Meek & Larson, 2019) and 48 USD for custom exome capture (Puritz & Lotterhos, 2018). For organisms with smaller genome sizes, lcWGS can be cheaper than reduced-representation approaches, and prices are likely to drop further as sequencing costs continue to decrease.

170 **2.2. Library preparation**

171 In most cases, Pool-seq approaches remain the most cost-effective way to obtain genome-wide
172 population-level data because it only requires preparation of a single sequencing library per
173 population. The obvious downside is that all individual-level information is lost, precluding many
174 types of analysis. Despite this limitation, Pool-seq has gained popularity because preparation of
175 individually indexed libraries for hundreds of samples used to be labor-intensive and costly (the
176 costs for preparing hundreds of libraries could easily outweigh the cost of sequencing). LcWGS
177 has now become a viable alternative because of the development of cheap library preparation
178 methods with efficient workflows that make it both practical and affordable to process hundreds
179 of samples (see Table S1 for an overview of methods used in recent LcWGS studies).
180 Therikildsen & Palumbi (2017), for example, describe a robust easy-to-implement protocol based
181 on reduced reaction volumes of Illumina's Nextera kit, which brings per-sample reagent costs
182 down to ~8 USD (based on current reagent pricing). Several other protocols that stretch
183 reagents in commercial kits reach similar price points (e.g. Gaio et al., 2019; Li et al., 2019). An
184 advantage of commercial kit-based protocols is that they often work "straight out of the box" or
185 require only limited optimization. Substantial further cost savings can be achieved with protocols
186 based on in-house expression and purification of *tn5* transposase (the enzyme used in
187 Illumina's Nextera tagmentation approach), such as described by Picelli et al., (2014) and
188 Hennig et al., (2018). With those protocols, per-sample library costs can be brought to <<1
189 USD, substantially reducing overall project costs when analyzing hundreds of samples and
190 essentially eliminating the added cost of individually indexed libraries, making total costs for
191 LcWGS equivalent to Pool-seq for similar total sequencing effort per population.

192
193 LcWGS library preparation methods also tend to be very efficient and scalable. For example,
194 *tn5* (tagmentation)-based protocols (like the one used by Therikildsen & Palumbi 2017) make it
195 possible to prepare 96 libraries in <5 hours (with <3 hours hands-on time) - substantially less
196 time than needed for most RAD-seq protocols (Meek & Larson, 2019). The Therikildsen and
197 Palumbi (2017) protocol also works well for relatively degraded DNA and requires only very
198 small amounts of input DNA (~2.5 ng). For highly degraded DNA, we have had great success
199 with the Carøe et al. (2018) single-tube method. Other cost-effective protocols produce
200 successful LcWGS libraries even from picogram-levels of input DNA (Hennig et al., 2018; Meier,
201 Salazar, Kučka, Davies, & Dréau, 2020; Picelli et al., 2014), for example enabling high
202 throughput production of libraries from individual zooplankters (Beninde, Möst, & Meyer, 2020).
203 Methods that sidestep DNA extraction with tagmentation directly on cells or tissue may lead to
204 additional efficiencies for LcWGS library preparation in the future (Vonesch et al., 2020).

207 **2.3. The need for a reference genome**

208 For non-model organisms, a key constraint associated with LcWGS is the need for a reference
209 genome to map the short-read sequence data generated from each individual. If a reference
210 genome is not already available for the species of interest, a common solution is to map to a
211 reference genome of a related species. While this can work well in some contexts, increasing
212 phylogenetic divergence between the re-sequenced species and the reference genome can
213 restrict mapping to the genomic regions that are most conserved between the two taxa and bias

214 estimates of population genomic parameters (Bohling, 2020; Nevado et al., 2014). Major
215 differences in genome organization (e.g. structural and copy number variants) can also exist
216 even between closely related species (Ekblom & Wolf, 2014). For these reasons, a species-
217 specific reference sequence is preferable where it can be obtained.

218
219 As a shortcut to obtaining species-specific reference sequence without de novo assembling a
220 full genome, Therkildsen and Palumbi (2017) mapped lcWGS reads to a reference
221 transcriptome, in practice performing 'in-silico' exome capture. However, major advances in
222 affordable long-read sequencing, powerful genome scaffolding techniques, and improved
223 assembly algorithms now enable chromosome-scale assemblies at a much lower cost and
224 faster speed than earlier approaches (reviewed by Rice & Green (2019)), facilitating high-quality
225 assemblies of mammalian-sized genomes (several Gb) with chromosome-length scaffolds for
226 as little as 1,000 USD (Dudchenko et al., 2018; Gatter, von Löhneysen, Drozdova, Hartmann, &
227 Stadler, 2020). Therefore, at this point, it probably makes sense to start most new lcWGS
228 studies with a de novo genome assembly or upgrade, if a reference sequence of sufficient
229 quality is not available.

230
231

232 **BOX 1: Glossary**

233

234 **Base quality score:** A metric associated with each base (nucleotide) in a sequencing read that
235 indicates the probability that the base is called incorrectly.

236

237 **Bayesian inference:** A statistical inference strategy that estimates model parameters by
238 characterizing its posterior probability distribution (i.e. $P(\text{parameter} \mid \text{data})$). By the Bayes
239 theorem, the posterior probability is formulated as a product of the likelihood function and the
240 prior probability distribution (probability distribution of model parameters before considering the
241 data) divided by the marginal probability of the data (which is a constant), i.e. $P(\text{parameter} \mid$
242 $\text{data}) = P(\text{data} \mid \text{parameter}) * P(\text{parameter}) / P(\text{data})$

243

244 **Genotype dosage:** The expected count of an allele in an individual. For a diploid individual, the
245 genotype dosage of the B allele = $P(AA \mid \text{data}) * 0 + P(AB \mid \text{data}) * 1 + P(BB \mid \text{data}) * 2$, where A
246 and B represent the two alleles at the site, and e.g. $P(AB \mid \text{data})$ represents the posterior
247 probability of the heterozygous genotype.

248

249 **Genotype imputation:** A method to infer missing genotypes and bolster genotype likelihood
250 estimation by identifying stretches of haplotypes shared between individuals.

251

252 **Genotype likelihoods (GLs):** The probability of observing the sequencing data at a certain site
253 in an individual given that the individual has each of the possible genotypes at this site (e.g. for
254 diploids there are 10 possible genotypes, which can be reduced to 3 if the major and minor
255 alleles are known), i.e. $P(\text{data} \mid \text{genotype})$, or $L(\text{genotype})$.

256

257 **Genotype likelihood (GL) model:** The mathematical model used to compute GLs. Different GL
258 models are built under different assumptions about the data, in particular about the sequencing
259 error profile. For example, the GATK model assumes that the sequencing quality scores
260 accurately capture the probability of sequencing error, and that all errors are independent. In
261 comparison, the Samtools model assumes that once a first error occurs at a certain site in an
262 individual, subsequent errors are more likely to occur at this site.

263
264 **Low-coverage whole genome sequencing (lcWGS):** We use this term to refer to whole
265 genome re-sequencing of individuals (i.e. labeled with unique barcodes) with depth too low to
266 reliably call genotypes without imputation (<5x). Note, however, that even for medium
267 sequencing depth (5-20x), inference accuracy may improve under a probabilistic analysis
268 framework based on GLs, rather than working with called genotypes (Nielsen et al., 2011).

269
270 **Mapping quality score:** A metric associated with each sequencing read aligned to the
271 reference genome that indicates the probability that the read is aligned to the correct position in
272 the reference sequence.

273
274 **Maximum likelihood inference:** A statistical inference strategy that estimates model
275 parameters by choosing the parameters that maximize the likelihood of the data. In other words,
276 the maximum likelihood estimators of model parameters = $\text{argmax}(L(\text{parameter}))$

277
278 **Posterior genotype probability:** The probability of an individual having one of the possible
279 genotypes at a certain site given the sequencing data, i.e. $P(\text{genotype} \mid \text{data})$.

280
281 **Prior genotype probability:** The probability of an individual having one of the possible
282 genotypes at a certain site before considering the sequencing data for this individual at this site,
283 i.e. $P(\text{genotype})$. The prior genotype probability can be uniform (i.e. all genotypes are equally
284 likely to occur), or can be informed by the allele frequency or the site frequency spectrum (SFS)
285 at this site for all individual samples. It is often used for the estimation of posterior genotype
286 probability in Bayesian inference.

287
288 **Restriction site-associated DNA sequencing (RAD-seq):** A group of techniques for
289 sequencing short flanking regions around restriction enzyme cut sites to obtain random samples
290 of genetic markers across the entire genome. These markers are typically sequenced at high
291 depth (e.g. >20x) for each individual so that individual genotypes can be confidently determined.

292
293 **Sample allele frequency (SAF) likelihood:** The probability of observing sequencing data at a
294 certain site across all individual samples given each possible sample allele frequency at this site
295 (e.g. for diploids, the possible sample allele frequencies range from 0 to 2n; n=sample size), i.e.
296 $P(\text{data} \mid \text{sample allele frequency})$.

297
298 **Whole genome sequencing of pools of individuals (Pool-seq):** A whole genome sequencing
299 strategy in which unlabeled DNA from multiple individuals is pooled before sequencing. The
300 sequencing depth is typically low on a per-individual level but high for each pool (e.g. >50x).

301 Due to the absence of individual barcodes, all individual-level information is lost in the
302 sequencing data.

303
304

305 **3. The toolbox: What types of analysis can we do with low-coverage** 306 **data?**

307

308 The major challenge in working with lcWGS data is that individual genotypes cannot be
309 accurately inferred (Li, Sidore, Kang, Boehnke, & Abecasis, 2011; Nielsen et al., 2012, 2011).
310 Many analytical tools that incorporate uncertainty about individual genotype calls have therefore
311 been developed in recent years, covering a broad diversity of common types of population
312 genomic inference. We here briefly introduce the most widely used applications (see Table 2 for
313 a more comprehensive list and the Supplementary Text Part 3 for additional details) and also
314 provide a tutorial with example data as a starting point for exploration:

315 <https://github.com/nt246/lcWGS-guide-tutorial>.

316

317 Currently, the most widely used program for lcWGS analysis is ANGSD (Korneliussen,
318 Albrechtsen, & Nielsen, 2014), a comprehensive package that implements an extensive variety
319 of analysis options. Because of its broad use and versatility, ANGSD will feature prominently in
320 this section's overview of available tools. However, we also seek to highlight that a variety of
321 alternative programs are available for most types of analysis (Table 2).

322

323 **3.1. Accounting for genotype uncertainty**

324 The most common way to incorporate uncertainty about true genotypes is to use genotype
325 likelihoods (GLs) rather than genotype calls in downstream analyses. A GL reflects the
326 probability of observing the sequencing reads that cover a specific site in an individual if said
327 individual has a particular genotype at this site. GLs refer to the set of likelihoods computed for
328 each of all the possible genotypes that individual could hold at that site (e.g. for diploids there
329 are ten possible genotypes: AA, AC, AG, AT, CC, CG, CT, GG, GT, and TT, which can be
330 reduced to three possible genotypes if the major and minor allele at a site are known, i.e. major-
331 major, major-minor, minor-minor).

332

333 The key factors that prevent us from confidently identifying the true genotype with lcWGS data
334 are uncertainties about 1) whether both alleles of a diploid individual have been sampled in the
335 stochastic sequencing process, 2) whether the base call (A, C, G, or T) at each position of a
336 sequencing read is correct, and 3) whether sequencing reads have been mapped to the correct
337 position in the genome. Several different models have been proposed for how the first two
338 sources of uncertainty should be accounted for in estimation of GLs (to our knowledge, no
339 current models directly factor in mapping accuracy). Currently, the most commonly used GL
340 models are probably the GATK model (McKenna et al., 2010) and the Samtools model (Li,
341 2011; Li et al., 2009) implemented in ANGSD (Korneliussen et al., 2014). The key difference
342 between these two GL models is that the GATK model assumes sequencing errors are
343 independent, whereas the Samtools model assumes a correlated error structure.

344

345

346 Unfortunately, the effects of GL model choice on downstream analyses are still incompletely
347 understood and likely depend on a diversity of factors including the accuracy of base calling and
348 base quality scores, the sequencing depth, and the type of inference sought. In our comparative
349 assessment (Section 4), we found that many types of analysis gave nearly identical results with
350 the GATK and the Samtools models, (Figure S4-S7), but that GL model choice can strongly
351 influence the number of rare alleles estimated from simulated low-coverage ($\leq 2x$) data (Section
352 4.1, see also Korneliussen et al., 2014 for a similar finding). However, more research is needed
353 to compare the performance of different GL models, and in the meantime, it may be prudent to
354 compare inference with several different GL models with a subset of the data for each new
355 dataset, particularly for analyses that rely on rare alleles.

356

357 On a related note, while base quality scores should reflect the probability of each called base in
358 a sequencing read being incorrect, it is widely recognized that instrument-reported values can
359 sometimes be inaccurate (i.e. poorly predicting the true frequency of sequencing errors;
360 Callahan et al., 2016; Ni & Stoneking, 2016). Given the central importance that base quality
361 scores typically play in estimating GLs when coverage is low, miscalibrated scores can
362 potentially bias inference, especially related to rare alleles (Kousathana et al. 2017). It may
363 therefore be advantageous to recalibrate base quality scores by first identifying putative
364 sequencing errors in the data and then adjusting the base quality scores based on the observed
365 error rates and patterns. This type of recalibration can be performed as an extra data
366 preprocessing step but is also implemented in some GL models (e.g. the SOAPsnp model in
367 ANGSD). Unfortunately, some of the most widely used methods (e.g. those implemented in
368 GATK and ANGSD; Auwera & O'Connor, 2020; Li et al., 2009) require a database of known
369 variable sites, which is not available for most organisms, and inputting an inaccurate variant
370 database can sometimes inadvertently result in further miscalibration of quality scores (Orr
371 2020). For non-model species, there may be more promise in approaches based on synthetic
372 spike-ins (e.g. PhiX; Zook et al., 2012; Ni & Stoneking, 2016) or monomorphic genomic regions
373 (e.g. sex chromosomes, ultra-conserved elements, or organellar DNA; Kousathana et al. 2017)
374 for which no true genetic variation is expected and sequencing errors can more readily be
375 identified. Other recently proposed techniques based on k-mer analysis (Orr, 2020) or
376 comparison of quality score profiles (Chung & Chen, 2017) also sidestep the need for a variant
377 database. However, none of these methods have yet been extensively validated for low-
378 coverage data. For now, a conservative approach may be to filter out bases with low quality
379 scores, but that results in data loss and does not fully address the issue of potential
380 miscalibration, so more research in this area is needed.

381

382 **3.2. From raw reads to SNP identification**

383 The initial steps in processing lcWGS data are similar to those used in many other NGS
384 approaches, such as high-coverage whole genome sequencing and Pool-Seq (Figure 2). These
385 include trimming adapter sequence and bases with low quality scores, mapping (aligning) reads
386 to a suitable reference genome, removing poorly mapped and duplicated reads, and -
387 depending on requirements of downstream tools - potentially clipping overlapping sections of
388 read pairs and realigning reads that span indels (see e.g. Therkildsen & Palumbi 2017). It is in

389 the downstream processing of the resulting filtered bam files that high-coverage and low-
390 coverage workflows diverge and where a probabilistic framework based on GLs becomes
391 central for low-coverage data.

392
393 The optimal approach in a GL-based framework would arguably be to always compute GLs for
394 every site in the genome, including sites that appear to be invariant in a sample (because with
395 lcWGS data we cannot be completely confident that we have not missed an alternative allele in
396 one or more of our samples). While this approach is required for some types of analysis (e.g. all
397 estimates of genetic diversity and the site frequency spectrum), other types of analysis (e.g.
398 analysis of population structure or outlier scans) are more tractable and computationally efficient
399 if only polymorphic sites are considered. Thus, a more practical solution for those types of
400 analysis is to initially identify likely polymorphic sites and restrict downstream GL-based
401 inference to those sites.

402
403 Although many types of genetic variants exist, lcWGS analysis has so far typically only
404 considered bi-allelic single-nucleotide polymorphisms (SNPs). A range of different programs can
405 identify SNPs from lcWGS data (Table 2). Because of built-in integration of a broad variety of
406 downstream analysis tools, ANGSD is often a convenient option. ANGSD identifies SNPs as
407 sites with minor allele frequencies significantly larger than zero. In this case, the number of
408 alleles at each site is restricted to two (major and minor allele), with the identities of these alleles
409 either determined through a maximum likelihood approach, setting the more common allele as
410 the major allele (Jørsboe & Albrechtsen, 2019; Skotte, Korneliussen, & Albrechtsen, 2012) or by
411 user specification (e.g. setting the reference or ancestral allele as the major allele). ANGSD
412 currently does not allow for identification of indels or multi-nucleotide polymorphisms, but users
413 could potentially identify bi-allelic indels with a different tool, such as Freebayes (Garrison &
414 Marth, 2012) or GATK (McKenna et al., 2010), and import estimated GLs into ANGSD for use in
415 downstream analysis. Regardless of the program used, quality control filters can be crucial to
416 ensure data reliability. Table 3 provides an overview of key filters that should be considered for
417 different types of analysis with lcWGS data.

418

419 **3.3. Individual-level analyses**

420 Despite the lack of called genotypes, lcWGS data can be used for a wide range of individual-
421 level analyses, which we define as those that do not require a priori grouping of individual
422 samples. It should be noted that the input formats for the different approaches differ between
423 programs and that in some cases SNP identification can be performed as part of the analyses
424 (see specific manuals). Note also that none of the analyses listed in this subsection are possible
425 with Pool-seq data.

426

427 **Population structure:** A key component of many population genomic studies is to characterize
428 population structure, using dimensionality reduction (e.g. PCA and PCoA) and/or model-based
429 clustering (e.g. admixture analysis). Dimensionality reduction methods are based on a
430 covariance matrix (PCA) or distance matrix (PCoA). Several methods for computing these
431 matrices while accounting for genotype uncertainty have been implemented. ANGSD, for
432 example, can either randomly sample one read per individual per site or use the most common

433 allele to represent the individual's allele frequency at this site (as either 0 or 1) and then
434 calculate the covariance and distance between every pair of individuals from these allele
435 frequencies. This simple approach has been shown to work well for datasets with very low
436 sequencing depth and uneven coverage across samples (see Section 4.2 and the ANGSD
437 manual). PCAngsd (Meisner & Albrechtsen, 2018), in contrast, estimates the covariance matrix
438 from GLs while taking population structure into account.

439
440 Model-based clustering methods that estimate admixture proportions of each sample assuming
441 a model of discrete ancestral populations are also implemented in several software programs
442 using GLs as input. These include NGSAdmix (Skotte, Korneliussen, & Albrechtsen, 2013) and
443 Ohana (Cheng, Racimo, & Nielsen, 2019) that both adopt a maximum likelihood implementation
444 of the classic STRUCTURE model (Pritchard, Stephens, & Donnelly, 2000; Tang, Peng, Wang,
445 & Risch, 2005), but differ in their optimization approaches. PCAngsd implements admixture
446 analysis with a different approach, which uses an intermediate output from its PCA analysis as a
447 starting point for model-based clustering. PCAngsd has been shown to outperform NGSAdmix
448 in runtime without strongly compromising its inference accuracy, making it potentially more
449 suitable for larger datasets (Meisner & Albrechtsen, 2018).

450
451 **Selection scans:** Several of the mentioned clustering programs also implement selection scan
452 approaches that do not require a priori grouping of individuals, as their general strategy is to
453 locate outlier loci that exhibit patterns of genetic variation among individuals that are highly
454 different from the genome-wide average. For example, PCAngsd (Meisner & Albrechtsen, 2018;
455 Meisner, Albrechtsen, & Hanghøj, 2021) implements the FastPCA method by Galinsky et al.
456 (2016) in a GL framework and in Ohana, SNPs that exhibit a significantly different covariance
457 structure can be identified as potentially under selection.

458
459 **Genome-wide association studies (GWAS):** Multiple statistical frameworks have been
460 developed to take genotype uncertainty into account in scans for genotype-phenotype
461 associations. GWAS often require large sample sizes to gain sufficient power, and a lcWGS/GL-
462 based approach provides an opportunity to maximize the number of individuals studied in a
463 cost-efficient way. Several GL-based GWAS approaches implemented in ANGSD have shown
464 power to discover meaningful associations, including in the presence of population structure
465 (Jørsboe & Albrechtsen, 2019; Skotte et al., 2012). These methods range from simple case /
466 control associations for identifying variants associated with binary phenotypes (Kim et al., 2011)
467 to analysis of quantitative traits with incorporation of covariates (Skotte et al. 2012; Jørsboe &
468 Albrechtsen 2019). The maximum likelihood approach recently developed by Jørsboe &
469 Albrechtsen (2019) also explicitly estimates the effect size of each locus.

470
471 **Linkage disequilibrium (LD):** LD estimation has many important applications, for example
472 relating to inference of population size, demographic history, selection, and discovery of
473 structural variants (Slatkin, 2008). In addition, since many downstream analyses make
474 assumptions about the independence of genomic loci, LD estimation is essential for excluding
475 strongly linked loci from a dataset (i.e. LD pruning). Several approaches have been developed
476 to estimate LD from GLs (i.e. taking genotype uncertainty into account), implemented e.g. in

477 GUS-LD (Bilton et al., 2018) and ngsLD (Fox, Wright, Fumagalli, & Vieira, 2019). Unfortunately,
478 the computational complexity of GUS-LD is too high for it to be practical for whole genome data,
479 but ngsLD has a more efficient algorithm and has different built-in functionalities to reduce its
480 computational complexity (e.g. restricting LD estimation between SNPs within a set distance,
481 setting a minor allele frequency filter, etc.), and comparative evaluation has indicated that
482 ngsLD tends to show less bias at low read depths (1-2x) than GUS-LD (Bilton et al., 2018; Fox
483 et al., 2019).

484
485 **Other types of analyses:** In addition to the examples discussed above, many other specialized
486 software packages have been developed to account for genotype uncertainty in various types of
487 inference, including estimation of relatedness among individuals (Korneliussen & Moltke, 2015;
488 Link et al., 2017), parentage inference (Whalen, Gorjanc, & Hickey, 2019) and pedigree analysis
489 (Snyder-Mackler et al., 2016), estimation of individual inbreeding coefficients (Link et al., 2017;
490 Vieira, Fumagalli, Albrechtsen, & Nielsen, 2013) and identity-by-descent tracts (Vieira,
491 Albrechtsen, & Nielsen, 2016), tests for introgression such as computation of ABBA-BABA/D-
492 statistics (Korneliussen et al., 2014), and construction of linkage maps (Rastas, 2017). More
493 examples are listed in Table 2. It is also important to note that samples sequenced at low-
494 coverage of the nuclear genome typically have very high sequencing depth across the
495 mitochondrial genome due to its much higher copy number in each cell, enabling recovery of
496 high-confidence full mitochondrial genome sequences for each individual (see e.g. Therkildsen
497 & Palumbi 2017). LcWGS thus provides a cost-effective way to generate full mitochondrial
498 genome sequences for hundreds of individuals, enabling unprecedented resolution for
499 phylogeographic analysis (Lou et al., 2018; Margaryan et al., 2020).

500
501

502 **3.4. Population-level analyses**

503 When individual samples can be grouped into discrete populations or categories based on
504 either prior information (e.g. sampling location or experimental treatment) or results from
505 individual-level population structure analyses (e.g. model-based clustering), analyses can be
506 conducted at the population level.

507

508 **Allele frequency estimation:** The estimation of population-specific allele frequencies is
509 essential for most population genomic studies as it is a required input for many downstream
510 analyses. Many programs, such as ANGSD (implementing the method of Kim et al., 2011) or
511 ATLAS (Link et al., 2017), can estimate minor allele frequencies for each site using a maximum-
512 likelihood or Bayesian approach. In programs where population-specific estimates are obtained
513 by running the program on each population separately (e.g. ANGSD), it is crucial for users to
514 explicitly define the same alleles as major and minor in all populations to avoid inadvertently
515 computing the frequency of opposite alleles in different populations.

516

517 **Site frequency spectrum (SFS):** The population-specific SFS is another population genomic
518 parameter essential for many downstream analyses. A challenge in estimating the SFS with
519 low-coverage data is that low-frequency SNPs are less likely to be identified as polymorphic and
520 therefore an SFS directly estimated from allele frequencies at identified SNP positions can be

521 biased towards intermediate frequencies. To get around this issue, ANGSD estimates the SFS
522 by using the sample allele frequency (SAF) likelihoods to formulate the likelihood function of the
523 SFS, which the program then optimizes (Nielsen et al., 2012). Depending on the availability of
524 an outgroup or ancestral reference genome, the inferred SFS can either be folded or unfolded
525 and ANGSD can estimate the SFS jointly for up to four populations (Korneliussen et al., 2014).
526 This probabilistic approach can correct for the bias caused by low-coverage data, but its
527 performance can be sensitive to the choice of underlying GL model (Korneliussen et al., 2014,
528 see also Section 4.1). Another important limitation is that the runtime of the SFS estimation
529 algorithm currently implemented in ANGSD grows quadratically with the number of samples and
530 it can become impractical to run across the whole genome if the sample size is very large. One
531 strategy is to estimate SFS by chromosome or in smaller windows and sum them up in the end.
532 Implementation of a faster algorithm (Han, Sinsheimer, & Novembre, 2015) may also be
533 included in future ANGSD releases (Fumagalli, personal communication).

534

535 **Genetic diversity and neutrality test statistics within a single population:** Derived
536 estimators of genome-wide genetic diversity θ , such as nucleotide diversity π and Watterson's
537 estimator, can be directly calculated from the population-specific SFS. These estimators of θ
538 can also be computed within genomic windows from window-specific SFS and subsequently,
539 different neutrality test statistics (e.g. Tajima's D) that evaluate the skewness of SFS in each
540 genomic window can be calculated. Individual heterozygosity estimates can be obtained by
541 estimating the SFS for individuals (rather than populations). All these diversity statistics can be
542 computed based on an infinite sites model implemented in ANGSD. In contrast, ATLAS (Link et
543 al., 2017) bases its θ estimation on a model that allows for back mutations (Felsenstein, 1981),
544 which can be more appropriate when working with ancient samples. Regardless of the method
545 used, it is important to note that when generating diversity estimates, non-variable sites should
546 be included in the calculation, and therefore minimum minor allele frequency filters or SNP p-
547 value filters should not be used.

548

549 **Genetic differentiation between populations:** In addition to estimates of *within*-population
550 diversity, the genetic differentiation *between* populations can be estimated with a variety of
551 different statistics, from simply quantifying the allele frequency difference to more complex
552 statistics such as relative genetic differentiation (F_{ST}) and absolute genetic divergence (d_{xy}).
553 Various estimators of F_{ST} can be computed from GL data using ANGSD, ngsTools (Fumagalli,
554 Vieira, Linderoth, & Nielsen, 2014), or vcflib (Garrison et al., 2021; see the Supplementary Text
555 Part 3 for more detail). vcflib can also estimate pF_{ST} , which, contrary to what the name suggests,
556 is not an F_{ST} estimator, but a statistic that quantifies the significance of allele frequency differences
557 between populations in face of genotype uncertainty (Domyan et al., 2016). In contrast to F_{ST} , no
558 established method to estimate d_{xy} from GLs has, to our knowledge, been included in major
559 software packages. Various custom scripts have been shared (see e.g.
560 <https://github.com/mfumagalli/ngsPopGen/tree/master/scripts>,
561 https://github.com/marqueda/PopGenCode/blob/master/dxy_wsfs.py). Note, however, that d_{xy} may
562 be over-estimated with these scripts so they should be used only for inspecting the relative
563 distribution of d_{xy} across the genome (Foote et al., 2016) and not to make inferences based on its
564 absolute values.

565
566
567
568
569
570
571
572
573
574
575
576
577
578
579
580
581
582
583
584
585
586
587
588
589
590
591
592
593

Other analyses based on derived statistics: In addition to the methods that work directly with GLs, many other types of population-level analysis can be conducted based on the derived statistics mentioned above. For example, several commonly used software tools can use allele frequency matrices as input to infer population relationships and potential gene flow (e.g. Treemix (Bradburd, Coop, & Ralph, 2018; Pickrell & Pritchard, 2012) and conStruct (Bradburd et al., 2018; Pickrell & Pritchard, 2012)), perform selection scans (e.g. BayPass (Gautier, 2015), WFABC (Foll & Gaggiotti, 2008; Foll, Shim, & Jensen, 2015)), association analyses (e.g. BayPass, LFMM2 (Caye, Jumentier, Lepeule, & François, 2019)), or variance partitioning analyses (e.g. RDA (Forester, Lasky, Wagner, & Urban, 2018)). To run these programs, population-level allele frequencies are estimated as explained above (e.g. using ANGSD), but have to be transformed into the appropriate input format using custom scripts. Similarly, the population-specific or multi-dimensional SFS estimated from ANGSD can be used to infer demographic history (e.g. with $\delta a \delta i$ (Gutenkunst, Hernandez, Williamson, & Bustamante, 2009) or fastsimcoal2 (Excoffier & Foll, 2011)), or to explicitly control for the effect of demography in selection scans (e.g. SweepFinder2 (DeGiorgio, Huber, Hubisz, Hellmann, & Nielsen, 2016)). Both locus-specific neutrality test statistics and F_{ST} values can be used in selection scans (e.g. OutFLANK (Whitlock & Lotterhos, 2015)), and genome-wide F_{ST} estimates can be used, for example, to test for isolation by distance (Mantel test) or to estimate effective migration surfaces (e.g. EEMS (Petkova, Novembre, & Stephens, 2016)). Furthermore, Ancestry_HMM (Medina, Thornlow, Nielsen, & Corbett-Detig, 2018) and ancestryinfer (Schumer, Powell, & Corbett-Detig, 2020) can infer local ancestry across the genome without called genotypes, although they require detailed SNP information for reference populations. Using derived statistics as input data can be a powerful approach to expand the available toolbox for lcWGS. However, unlike the GL-based programs listed in the rest of this section and Table 2, this approach does not carry uncertainty about parameter estimation downstream. Accordingly, if summary statistics rather than GLs are used as input for analysis, p-values etc. should be interpreted with caution and in light of the expected precision given the sample size and sequencing depth (see Section 4).

594
595

596 **4. Experimental design: The tradeoffs between sequencing depth per** 597 **sample and total number of samples analyzed**

598
599
600
601
602
603
604
605
606
607

With a finite sequencing budget, do we learn more about a population from adding more sequencing depth to each individual or stretching the sequencing effort over more individuals? Several previous studies have used simulated data to address this question (e.g. Buerkle & Gompert, 2013; Fumagalli, 2013; Nevado et al., 2014). In general, these studies have found that sampling many individuals at 1x or 2x read depth provides more accurate estimates of many population parameters than higher read depth for fewer individuals. However, both the simulation (e.g. Haller & Messer, 2019; Huang, Li, Myers, & Marth, 2012) and the GL-based data analysis toolboxes (e.g. Fumagalli, Vieira, Linderoth, & Nielsen, 2014; Korneliussen et al., 2014; Meisner & Albrechtsen, 2018) have evolved rapidly since these studies were conducted,

608 and a more up-to-date evaluation is now needed. Here, we used simulated data to compare
609 common types of population genomic inference under a wide range of sample size and
610 sequencing depth combinations, including depths $<1x$, which were not explicitly evaluated in
611 earlier studies. Full details about all the simulations and analyses can be found in the
612 Supplementary Methods (Part 1) and Table S2, and our entire simulation and analysis pipeline
613 is available on GitHub (<https://github.com/therkildsen-lab/lcwgs-simulation>).
614

615 **4.1. Population genomic inference for single populations**

616 We used SLiM (Haller & Messer, 2019) to simulate an isolated population that has reached
617 mutation-drift equilibrium, and evaluated the accuracy of lcWGS (reads simulated with ART
618 (Huang et al., 2012)) for inferring key population genomic parameters, including allele
619 frequencies, the SFS, θ , Tajima's D (estimated with ANGSD (Korneliussen et al., 2014)), and
620 linkage disequilibrium (estimated with ngsLD (Fox et al., 2019)) under different experimental
621 designs.
622

623 As expected, the accuracy of allele frequency estimation consistently increases with both higher
624 sample size and depth of coverage per individual (as measured by the r^2 values in Figure 3).
625 The number of false negative SNPs (i.e. true SNPs in the population that fail to be identified)
626 similarly decreases with higher sample size and higher coverage per individual (Figure S1).
627 Importantly, however, distributing the same total sequencing effort (i.e. the product of sample
628 size and coverage per individual) across more samples, with each sample receiving lower
629 coverage (i.e. going from bottom left to top right in Figure 3) also consistently improves allele
630 frequency estimation, even when each sample is sequenced at a coverage as low as $0.25x$. The
631 increased accuracy arises because each allele is less likely to be sequenced more than once
632 with lower per-sample coverage, and thus the effective sample size gets higher.
633

634 Consistent with what the authors of ANGSD have previously shown (Korneliussen et al., 2014),
635 we found that for SFS-based inference, the choice of GL model used can strongly influence its
636 result. With the Samtools GL model, Watterson's θ is systematically underestimated when the
637 average coverage is low ($\leq 4x$), although Tajima's θ (π) estimates are more robust (Figure S2).
638 Consequently, Tajima's D tends to be overestimated (Figure S3). In contrast, when the GATK
639 GL model is used, Watterson's θ , Tajima's θ , and Tajima's D can all be accurately estimated
640 even at coverage as low as $0.5x$ (Figure S2, S3). The two GL models differ in performance
641 because both the GATK model and our simulation model assume that each base quality score
642 reflects an independent and unbiased measurement of the probability of sequencing error
643 (Huang et al., 2012; McKenna et al., 2010), whereas the Samtools model assumes that if one
644 sequencing error occurs at a certain locus, subsequent errors are more likely (Li, 2011; Li et al.,
645 2009). As a result, with the Samtools model, lower-frequency mutations are less likely to be
646 identified as polymorphic sites and more likely to be interpreted as sequencing errors when the
647 coverage is low. This leads to an underestimation of the number of singleton mutations when
648 using the Samtools model, and therefore Watterson's θ tends to be underestimated, at least for
649 our simulated data. We note, however, that these low-frequency SNPs have minimal impact on
650 many other types of population genomic analyses and, in fact, are often filtered out. Consistent
651 with this, we did not observe any strong discrepancies between the two GL models in other

652 types of analysis that we performed in this study (Figure S4-S7). We also stress that the
653 sequencing errors modeled in our simulations may not accurately represent the sequencing
654 error profile in real life, so our result should not be interpreted as a recommendation of one GL
655 model over the other.

656

657 For LD estimation, we found that relative estimates (which may be adequate for many uses, e.g.
658 for the identification of LD blocks or LD pruning) could be reliably obtained with per-sample
659 coverage as low as 1-2x. However, higher per-sample coverage (e.g. $\geq 4x$) is required to get
660 precise and accurate absolute estimates of LD (e.g. for use in demographic inference) even with
661 sample size as large as 160 (Figure S4, S5, Fox et al. 2019).

662

663

664 **Box 2. Performance of lcWGS vs. Pool-seq in allele frequency** 665 **estimation**

666 A key advantage of lcWGS over Pool-seq is that each sequencing read can be assigned to an
667 individual so we can detect uneven sequencing coverage and account for it in parameter
668 estimation. But does that matter in practice if the contribution of each individual to the
669 sequencing pool is roughly equal? With our simulated data, we found that a lcWGS analysis
670 approach that accounts for individual-level GLs consistently provides slightly more accurate
671 allele frequency estimates than Pool-seq analysis (which ignores individual-level information)
672 even when all individuals contribute equally to the sequencing pool (Figure 4). This is because
673 the sampling variance inherent to next-generation sequencing creates stochastic variation in the
674 sequencing depth for each individual at each locus (so some by chance will be overrepresented
675 while others will be underrepresented). In practice, inaccuracies due to measurement and
676 pipetting errors, variation in DNA quality, and sequencing biases make it almost impossible to
677 ensure the optimal scenario of even amounts of sequences among samples (Figure S8, see
678 also Schlötterer, Tobler, Kofler, & Nolte, 2014), further enhancing the value of being able to
679 account for sample overrepresentation with individually barcoded reads (Figure S9, S10).

680

681

682 **4.2. Inference of spatial structure**

683 To evaluate the power of different lcWGS sampling designs in detecting population structure,
684 we simulated a metapopulation consisting of nine subpopulations located on a three-by-three
685 grid that have reached mutation-drift-migration equilibrium. We first examined a scenario in
686 which gene flow among subpopulations is low (0.25 effective migrants between neighboring
687 subpopulations per generation). In this scenario, the spatial structure among subpopulations
688 can be correctly inferred from PCA even with extremely low sample size (5 samples per
689 subpopulation) and coverage (0.125x coverage per sample; Figure 5A). In addition, migrant
690 individuals and hybrids, when included in the sample, can be identified in the PCA (Figure 5A),
691 which would not be possible with a Pool-seq design.

692

693 We then increased the level of gene flow (1 effective migrant between subpopulations every
694 generation). As expected, the power of PCA to resolve the weaker spatial structure slightly
695 declines, but interestingly, small sample size causes a greater loss of power than low coverage

696 does (Figure 5B). Subpopulations fail to form discrete clusters in PCA space when the sample
697 size per population is 5, unless the coverage is 2x or higher per sample. On the other hand, with
698 a sample size of 10, the correct spatial structure can be inferred with a coverage as low as
699 0.125x (i.e. a per-population coverage of only 1.25x; Figure 5B). The reason why we can push
700 the per-sample coverage so low is that PCA depends on reliable covariance estimation between
701 some, but not all pairs, of samples in the dataset. To get reliable covariance estimates in a
702 sample pair, both samples need to have at least 1x coverage at some informative SNPs. As
703 sample size increases, the number of all available sample pairs increases quadratically, and the
704 number of sample pairs for which enough informative SNPs are shared also increases
705 quadratically. Therefore, the overall population structure is more likely to be correctly
706 extrapolated from these sample pairs. We also note that, due to computational limitations, our
707 simulations are based on only a single 30Mb chromosome. Since the power of PCA depends on
708 the number of informative SNPs shared between pairs of samples, with a larger genome size,
709 even lower sequencing depth and/or sample size would be required to resolve the spatial
710 structure among subpopulations, given the same SNP density as simulated here (see Figure
711 S11 for an example of this). Lastly, we found that the read sampling method implemented in
712 ANGSD (Korneliussen et al., 2014), the results of which are presented here, outperforms
713 PCAngsd (Meisner & Albrechtsen, 2018) in scenarios with low sample size (e.g. ≤ 10 samples
714 per population) or very low coverage (e.g. $\leq 0.25x$ per sample; Figure S12, S13).

715
716

717 **4.3. Scans for divergent selection in the face of gene flow**

718 A primary advantage of lcWGS compared to reduced-representation sequencing approaches is
719 the increased resolution in genome scans for signatures of selection, for example in the form of
720 outlier loci that show elevated levels of differentiation between populations or
721 elevated/depressed neutrality test statistics within a single population. To evaluate how
722 experimental design affects our ability to detect outliers, we simulated two populations
723 connected by gene flow that are strongly affected by divergent selection on a subset of loci. We
724 estimated per-SNP F_{ST} between the two populations, as well as Tajima's D and Fay and Wu's H
725 within one of the populations, from lcWGS data to identify the loci under selection (details in the
726 Supplementary Methods).

727

728 We first examined a scenario where the size of each population is large (the effective population
729 size (N_e) = 5×10^4) and gene flow is high (5 effective migrants per generation). In this scenario,
730 seven out of eight SNPs under divergent selection, along with their neighboring neutral SNPs,
731 show highly elevated F_{ST} values compared to the genome-wide background, creating a distinct
732 pattern of narrow genomic islands of divergence (Figure 6; Turner, Hahn, & Nuzhdin, 2005).
733 This F_{ST} landscape can be recovered from lcWGS data with a total sequencing coverage per
734 population as low as 10x (e.g. 40 samples per population and 0.25x coverage per sample,
735 Figure 6). For a given total sequencing effort, however, we observe an increase in background
736 F_{ST} when the sequencing is spread over fewer individuals (e.g. 5 samples per population and 2x
737 coverage per sample give more background noise than 40 samples each at 0.25x coverage),
738 which can lead to overestimated genome-average F_{ST} (Figure S7) and more false positive
739 signals in the outlier detection (Figure 6). With similar sequencing effort, most of these loci

740 under selection can also be identified by signals of decreased Tajima's D and Fay and Wu's H,
741 although the absolute values of these estimates are sensitive to both sample size and coverage
742 (Figure S14, S15). Unlike for F_{ST} , spreading the same sequencing effort across more samples
743 does not consistently improve the accuracy of these neutrality test statistics (as some require
744 higher coverage for accurate estimation). We also estimated F_{ST} and neutrality test statistics in
745 a scenario with smaller population size ($N_e = 10^4$) and lower gene flow (2.5 effective migrants
746 per generation), and the same general conclusions hold (Figure S16, S17).

747

748 **4.4. The optimal experimental design depends on study goals**

749 Perhaps unsurprisingly, our simulation results suggest that there is not a single lcWGS
750 experimental design that is ideal for all purposes. Instead, the optimal design depends on the
751 goals, system, and budget of a study. For many common types of population genomic inference
752 (e.g. allele frequency estimation, population structure analysis, genetic differentiation between
753 populations), higher accuracy can be achieved by spreading a given sequencing effort thinly
754 across more samples (Figures 3, 5, 6). There are, however, some notable exceptions. For
755 example, inference that depends heavily on low-frequency alleles (e.g. Watterson's θ , Tajima's
756 D) can be very sensitive to the chosen GL model when per-sample sequencing coverage is low,
757 so until we have a better understanding of which GL models best fit the empirical data,
758 sequencing each sample with relatively higher coverage (e.g. >4x) might generate more robust
759 results for these types of analyses (Figure S2, S3). Nevertheless, if relative measures of these
760 statistics are of interest rather than their absolute values (e.g. for outlier detection), lower
761 coverage of each sample may be adequate (Figure S14, S15). Similarly, the methods that are
762 currently available for LD estimation with lcWGS data can generate biased absolute estimates
763 when the coverage is lower than 4x (Figure S4, S5), but note that reliable relative estimates of
764 LD can be obtained at lower coverage.

765

766 It is important to keep in mind that tradeoffs exist between sample size and per-sample depth:
767 with a given budget, the higher per-sample sequencing depth needed for robust estimation of
768 the SFS (e.g. for demographic inference using $\delta a \delta i$) or absolute values of e.g. Tajima's D or LD
769 will likely compromise the accuracy for other estimates, e.g. of allele frequencies or F_{ST} outliers
770 (unless sample sizes are large even with the higher per-sample coverage). Accordingly,
771 researchers must carefully consider what types of inference are most essential to their study
772 goals and strike an appropriate balance. Based on our results here and those from previous
773 studies, we provide some general guidelines to lcWGS experimental design in Table 4. For
774 more targeted guidance, we also encourage researchers to build on our simulation pipeline
775 (<https://github.com/therkildsen-lab/lcwggs-simulation>) to optimize the experimental design for
776 their specific studies.

777

778 **Box 3. Performance of lcWGS vs. RAD-seq in selection scans**

779 Compared to lcWGS, RAD-seq has the advantage of generating high-confidence genotype
780 calls, but suffers from a sparser coverage of the genome, which can result in missed signals in
781 selection scans (Lowry et al., 2017). Here, we simulated RAD-seq data for our two divergent
782 selection scenarios with a range of realistic sample sizes and RAD tag densities. In the scenario
783 with larger population size and higher gene flow, we found that even with a large sample size

784 and a much higher marker density than typically used (128 RAD tag SNPs per Mb, i.e.
785 ~128,000 SNPs in a 1Gb genome), RAD-seq picked up some, but tended to miss several of the
786 narrow F_{ST} peaks. With a lower, much more commonly used marker density (e.g. 8 tags per Mb,
787 or ~8,000 SNPs in a 1Gb genome), the majority of the selection-induced peaks would be
788 missed, regardless of sample size (Figure 7). In the scenario where the population size is
789 smaller and gene flow is lower, RAD-seq is more likely to sample SNPs within the true F_{ST}
790 peaks due to the stronger linked selection, but because of the higher background noise in these
791 scenarios, it still struggles to detect distinct F_{ST} peaks (Figure S18). These findings are
792 consistent with a growing number of empirical examples where RAD-seq missed signatures of
793 selection clearly detected with WGS data (see the Introduction).

794
795

796 5. Application to empirical data

797

798 To supplement our simulation-based evaluation of lcWGS inference with an exploration of how
799 sequencing depth affects the identification of polymorphic sites, population structure analysis
800 and detection of outlier loci in empirical data, we subsampled and re-analysed previously
801 published whole genome sequencing data from the Neotropical butterfly *Heliconius erato* (Van
802 Belleghem et al., 2017). The *H. erato* radiation comprises several subspecies that show a vast
803 visual diversity in Müllerian mimicry related to wing patterns, and many of the underlying
804 candidate genes have been identified (Reed et al., 2011; Van Belleghem et al., 2017). For
805 example, the *optix* gene has been shown to control the red band phenotype in multiple
806 *Heliconius* species and accordingly shows strong differentiation among subspecies with
807 different band patterns (Reed et al., 2011; Van Belleghem et al., 2017). We subsampled
808 resequencing data (originally average coverage of $11x \pm 2.3x$ per individual) mapped to the *H.*
809 *erato demophoon* (v1) to coverage depths of 8x, 4x, 2x, 1x, 0.5x and 0.25x (see Supplementary
810 Methods (Part 1)) and analysed them in a GL framework. For simplicity, we focus on results for
811 8x, 2x and 0.5x coverage, as results from 4x and 1x are very similar to 8x and 2x, respectively
812 (see supplementary Figure S19).

813

814 First, we found a positive correlation between the number of variable sites identified during SNP
815 identification in ANGSD and the mean genome-wide sequencing coverage (Figure 8a; quadratic
816 function: $r^2 = 0.98$, $p=0.00099$). Across all 51 individuals used in the final analyses, the number
817 of SNPs identified with a p-value threshold of 10^{-6} ranged from 12,266 at 0.5x coverage to
818 14,851,731 at a mean coverage depth of 8x. It has to be noted though, that the number of
819 detected SNPs depends on the p-value threshold, and for a dataset with a mean per-individual
820 coverage of 0.25x a lower p-value threshold would have to be used to identify any SNPs at all
821 (Figure 8).

822

823 Second, we reconstructed the population structure using PCA, performed on covariance
824 matrices estimated using random read sampling in ANGSD (see Supplementary Methods). The
825 PCA showed a very similar clustering pattern for all datasets regardless of coverage level, with
826 populations grouping into three distinct clusters corresponding to the geographic origin of
827 samples (Central America, East of Andes, West of Andes; Figure 8b). One subspecies (*H. erato*

828 *hy dara*) sampled from two geographic regions was split over two clusters. On a finer population
829 structure scale, we observed a slightly wider spread of data points at the lowest coverage
830 (0.5x), although the general clustering was comparable to higher coverages.

831
832 Lastly, comparing the genetic differentiation between *H. erato* subspecies with (n=28) and
833 without (n=23) the red bar phenotype (Van Belleghem et al., 2017), we recovered the well-
834 characterized F_{ST} peak around the *optix* gene at per-individual coverages as low as 1x (Figure
835 8c; Van Belleghem et al., 2017). At 0.5x coverage, we were restricted to estimating F_{ST} within
836 fewer genomic windows compared to higher coverages (112 50kb windows at 0.5x vs 255 50kb
837 windows at >1x along scaffold 1801), leading to much sparser window coverage across the
838 scaffold and therefore a noisier signal (Figure 8c). However, even at this low resolution, we
839 detected one differentiated genomic window in the *optix* region, albeit the estimated F_{ST} was
840 elevated at 0.5x ($F_{ST} \sim 0.6$) compared to higher coverages ($F_{ST} \sim 0.4$).

841
842 Overall, these results suggest that even at a comparatively low individual sequencing coverage
843 of 0.5-1x and moderate sample sizes of 20-30 per population, we can detect population
844 structure and recover distinct peaks of differentiation across the genome in empirical data.

845

846

847 **Box 4. Using imputation to bolster genotype estimation from lcWGS**

848

849 The majority of current population genomic inference methods, including all the lcWGS methods
850 discussed in this paper so far, consider data on a SNP-by-SNP basis and accordingly ignore all
851 the information contained in the surrounding haplotype structure. Imputation can be used to
852 boost genotyping accuracy by leveraging LD patterns between variants to identify shared
853 stretches of chromosome and incorporate information from flanking alleles to infer missing or
854 low-confidence genotypes (Li et al., 2011; Pasaniuc et al., 2012). Imputation has been used
855 extensively to obtain genotype calls from low-coverage data in humans and agricultural species,
856 but has seen limited application in non-model species because most imputation methods, such
857 as Beagle (Browning & Yu, 2009) and findhap (VanRaden, Sun, & O'Connell, 2015), rely on
858 externally generated haplotype reference panels, which are unavailable for most species. In
859 contrast, the more recently developed program STITCH imputes directly from sequence read
860 data without reference panels, and has been shown to perform well when sample sizes are
861 large (n>2000; Davies, Flint, Myers, & Mott, 2016). However, sample sizes of this magnitude
862 are not achievable in many studies, especially for rare or elusive species. To evaluate the utility
863 of imputation without reference panels with sample sizes more typical of studies of non-model
864 species, we simulated three populations with varying levels of genetic diversity and LD, tested
865 combinations of sequencing depths and sample sizes, and identified the conditions under which
866 reference panel-free imputation is likely to bolster genomic analyses of lcWGS data.

867

868 **Imputed genotype accuracy**

869 We simulated three populations characterized by 1) low diversity, high LD ($N_e = 1,000$, $r = 0.5$
870 cM/Mb); 2) medium diversity, medium LD ($N_e = 10,000$, $r = 0.5$ cM/Mb); and 3) medium

871 diversity, low LD ($N_e = 10,000$, $r = 2.5$). For each population, we subsampled 25, 100, 250, 500
872 or 1000 individuals and simulated sequencing reads to average depths of 1x, 2x and 4x per
873 sampled individual. We compared genotype dosages for all SNPs with minor allele
874 frequency >0.05 imputed without reference panels in Beagle and STITCH, to those estimated
875 without imputation in ANGSD (see the Supplementary Text Part 1 and Table S2 for details on
876 simulations, genotype dosage estimation and imputation).

877
878 Our analysis suggests that using imputation without reference panels does improve population
879 genomic inference under certain circumstances. Imputation was most effective under the low
880 diversity, high LD scenario (Figure 9A). Under this scenario, genotype dosages imputed in
881 STITCH from large sample sizes ($n \geq 500$) sequenced at 1x coverage were highly correlated with
882 true genotypes ($r^2 > 0.94$), and all experimental designs with sample sizes ≥ 100 showed a
883 substantial improvement in genotype estimation (Figure 9A). In the medium diversity and
884 medium LD scenario, larger sample sizes were necessary to achieve similar imputation
885 accuracy (e.g., $n=1000$ was needed for $r^2=0.95$; Figure 9B). Performance was markedly worse
886 in the scenario with medium diversity and low LD, but there was nonetheless an improvement
887 when imputing from large sample sizes ($n \geq 250$) or greater sequencing depths ($\geq 2x$) compared
888 to genotypes called without imputation (Figure 9C).

889

890 **Considerations for using imputation in non-model systems**

891 Choosing whether to apply imputation to real-world data will depend on the details of the study
892 system and the experimental design. In general, imputation accuracy increases with SNP
893 density and LD between SNPs (de Bakker, Neale, & Daly, 2010; Shi et al., 2018), and our
894 results suggest that populations with lower LD (even those with greater SNP density) require
895 greater sample sizes and/or coverage to achieve the same imputation accuracy. For
896 populations with higher LD, STITCH can substantially boost genotype accuracy for samples
897 sequenced at 1x coverage, provided sample sizes are adequate ($n \geq 100$). When coverage is
898 higher ($\geq 2x$), Beagle tends to perform similarly to or even outperform STITCH. However, for
899 populations with lower LD, the improvement in genotype accuracy by imputation may be small
900 unless sample sizes are ≥ 1000 and/or coverage is $\geq 2x$ for the conditions tested here; at smaller
901 sample sizes or lower coverage, the potential benefit of imputation for low LD populations may
902 not warrant the computational time.

903

904 Imputation provides another potential benefit for spreading sequencing effort thinly among many
905 individuals in some circumstances. As our results have shown, by leveraging LD information
906 from all samples, imputation can to some extent make up for the genotype uncertainty inherent
907 in lcWGS data. For example, in the high LD population, genotypes imputed in STITCH from
908 1000 samples sequenced at 1x coverage were only slightly lower in accuracy ($r^2=0.975$) than for
909 500 samples at 2x coverage ($r^2=0.981$) and 250 samples at 4x coverage ($r^2=0.982$). For many
910 questions where a large sample size is necessary to achieve adequate power, such as GWAS,
911 what can be gained from increased sample size could readily outweigh the minimal loss in
912 genotype accuracy. In addition, for some GWAS methods, the remaining genotype uncertainty
913 can be incorporated directly into the analysis (Skotte et al., 2012; Jørsboe & Albrechtsen, 2019).

914

915 Because the performance of imputation varies with the LD and diversity of populations, a priori
916 information on population history may help researchers anticipate how well imputation will
917 perform. A set of “true genotypes” (e.g. from high-depth samples) and quality metrics output by
918 the imputation programs (Browning & Yu, 2009; Davies et al., 2016) can also be used.
919 Populations with small effective population size or that have experienced recent bottlenecks,
920 such as threatened or endangered species, will have higher genome-wide LD (Hayes, Visscher,
921 McPartlan, & Goddard, 2003; Waples & Do, 2010), making them potentially good systems for
922 applying imputation if relatively large sample sizes (e.g. ≥ 100 for the scenarios simulated here)
923 can be obtained. Where pedigree information is available, methods that incorporate the
924 pedigree into imputation can be used (e.g. Ros-Freixedes, Whalen, Gorjanc, Mileham, &
925 Hickey, 2020; Whalen, Ros-Freixedes, Wilson, Gorjanc, & Hickey, 2018). Finally, although
926 imputation has been mainly applied to regular short-read data, the haplotype reconstruction step
927 could be greatly simplified by long-read or linked-read data that is becoming increasingly
928 available (see Section 7).

929
930

931 **6. Current limitations and future developments**

932

933 Despite the many strengths of lcWGS, there are also clear limitations to this data type. Here, we
934 outline key constraints that researchers should consider before adopting the approach and
935 discuss prospects for overcoming these constraints in the future.

936

937 **Not suitable for analyses requiring genotype calls:** It is important to stress that the potential
938 for improved inference accuracy by spreading sequencing effort thinly over many individuals is
939 only realized if the resulting uncertainty about individual genotypes is accounted for statistically
940 in downstream analyses, with approaches such as those reviewed in Section 3. As discussed,
941 hard-calling genotypes from lcWGS data remains likely to bias inference regardless of how
942 large the sample size is, so lcWGS data is not well-suited for analysis types or downstream
943 software that require genotypes as input, unless imputation can provide more accurate
944 genotype calls (see Box 4 for details). However, as outlined in Section 3, GL-based inference
945 frameworks are available for most major types of population genomic analysis and many
946 additional approaches are under development. Alternatively, many researchers are now
947 embracing a hybrid approach, where they sequence a few samples at higher coverage in order
948 to conduct some analyses that require confident genotype calls, and perform the rest of their
949 analyses using lcWGS data from more samples (e.g. Foote et al., 2016; Liu et al., 2014;
950 Pečnerová et al., 2021; Westbury et al., 2018). Furthermore, another promising strategy with a
951 hybrid dataset is to form a reference panel using a subset of high-coverage samples, and
952 impute the genotypes of low-coverage samples (e.g. Fuller et al., 2020).

953

954 **Lack of user-friendly software interfaces and documentation:** Unfortunately, a key barrier to
955 the wider adoption of lcWGS has been a lack of user-friendly interfaces and sparse
956 documentation for programs that handle GL data. Accordingly, these tools are only accessible
957 to users with prior expertise in bioinformatics, and the development of workflows often requires
958 a substantial time investment. We hope that this beginner’s guide can be part of the effort to

959 increase the accessibility of lcWGS. We are also aware that efforts are underway to develop a
960 more user-friendly version of ANGSD, which should make this powerful and versatile software
961 package accessible to a broader set of researchers (Altinkaya and Fumagalli, personal
962 communication).

963

964 **Computational demands:** Another practical limitation is the often much greater computational
965 cost of probabilistic GL-based methods compared to methods based on called genotype. For
966 example, SFS estimation from GLs in ANGSD is computationally intensive with very large
967 sample sizes, which may be prohibitive for researchers without access to high-performance
968 computational resources. New, more efficient algorithms (e.g. Han et al., 2015) and strategies
969 for analyzing smaller sections of the genome in turn (see Section 3) may alleviate some of these
970 constraints, but the computational demands for analysis should definitely be considered,
971 especially for researchers transitioning to lcWGS after working with much smaller datasets such
972 as RAD-seq.

973

974 **Limitations and gaps in the current toolbox:** Although tremendous progress has been made
975 in the development of methods and tools for the analysis of lcWGS data over the past decade,
976 some key analytical challenges remain. One important issue is the potential sensitivity to the
977 choice of GL model in some types of analyses (see Section 4.1 and Box 4 in Fuentes-Pardo &
978 Ruzzante, 2017). A better understanding of which GL models best match the real error
979 structures generated by different sequencing platforms and more well-established methods for
980 base quality score recalibration is essential for more robust inference from low-coverage data.
981 In addition, alignment error is not taken into account in any of the current GL models, which
982 could be problematic for genomes with high repeat content or for poor-quality reference
983 genomes. The current analysis framework implemented in most software packages is also
984 centered on the analysis of diploid organisms; extension to an arbitrary ploidy level would
985 expand its usefulness for working with haploid and polyploid organisms, and key parts of this
986 framework have already been developed (Blischak, Kubatko, & Wolfe, 2018). There also remain
987 types of analysis for which GL-based methods are not yet available. However, new analytical
988 approaches for lcWGS data continue to emerge. For example, GL-based equivalents to some
989 established approaches, such as implementation of the Pairwise Sequentially Markovian
990 Coalescent (PSMC) model, are currently under development (ngsPSMC
991 [\[https://github.com/ANGSD/ngsPSMC\]](https://github.com/ANGSD/ngsPSMC)).

992

993 **Analysis susceptible to batch artifacts:** LcWGS data have great potential for reusability
994 because the possibility to combine different datasets does not depend on the selection of the
995 same restriction enzyme or markers. However, because of the low level of redundancy in the
996 data, lcWGS could be particularly susceptible to batch effects when different datasets are
997 combined. As mentioned earlier, some GL-based approaches are heavily dependent on
998 accurate modeling of the error structure in the data, which can vary between sequencing
999 batches. For example, the sequencing error rate could be overestimated in one batch and
1000 underestimated in another (Lou & Therikildsen, 2021), leading to artificial differences between
1001 batches that could confound real biological signals. Many of these batch effects can be

1002 mitigated with simple bioinformatic approaches, although extra care needs to be taken (Lou &
1003 Therkildsen 2021).

1004

1005 **Limited ability to phase lcWGS data:** A major limitation is that no bioinformatic solution is yet
1006 available to allow accurate phasing of lcWGS data without a reference panel, therefore
1007 prohibiting haplotype-based analyses. Haplotype data are a rich source of information, e.g. for
1008 inference of local ancestry tracks across the genome, demographic histories, or ongoing
1009 selective sweeps (see Leitwein, Duranton, Rougemont, Gagnaire, & Bernatchez, 2020) for a
1010 detailed overview). Despite major technological advances, long-read sequencing that can
1011 recover haplotype information remains too costly for typical population genomic studies.
1012 However, the recent development of an affordable linked-read low-coverage sequencing
1013 approach (Meier et al., 2021) promises to open many new opportunities for haplotype-based
1014 inference on a population scale by enabling efficient phasing and imputation of low-coverage
1015 linked-read data without a reference panel. Phased haplotype data will provide substantial
1016 improvement in imputation performance compared to the short-insert lcWGS data explored in
1017 Box 4, and make completely new types of analysis possible with lcWGS data.

1018

1019 **Limitations for small sample sizes and very large genomes:** LcWGS will not be an optimal
1020 solution for all study systems. In particular, for species that are rare or difficult to collect (e.g.
1021 endangered or elusive species), it may be impossible to obtain adequate sample sizes for
1022 accurately estimating population genomic parameters with lcWGS (see Section 4). In these
1023 cases, many types of analysis, such as demographic history, diversity, selective sweeps and
1024 inbreeding levels, can be performed based on deep sequencing of the genome of a few or even
1025 just a single individual (e.g. Li & Durbin, 2011). For species with extremely large genomes (e.g.
1026 many amphibians and pine species), whole genome sequencing may also remain impractical at
1027 any sequencing depth from a cost or data storage/handling perspective, and reduced
1028 representation approaches such as RAD-seq or targeted sequence capture may be preferable
1029 (Burgon et al., 2020; McCartney-Melstad, Mount, & Shaffer, 2016). Of note, however, for
1030 targeted methods like sequence capture, low-coverage sequencing of larger sample sizes and
1031 associated GL-based analysis can, similar to lcWGS, confer distinct advantages over
1032 sequencing fewer individuals at higher depth (e.g. Snyder-Mackler et al., 2016; Therkildsen et
1033 al., 2019; Warmuth & Ellegren, 2019; Wilder et al., 2020).

1034

1035

1036 **7. Conclusion**

1037 In conclusion, although some limitations still exist for the use of lcWGS, this approach offers
1038 many advantages over reduced-representation sequencing or pooled WGS approaches and is
1039 ripe for broader implementation. We are excited about how its cost-effectiveness democratizes
1040 population-scale whole genome analysis, which until recently was only available to well-funded
1041 research groups working on model species. The ability to obtain full genome data for hundreds
1042 of individuals even on modest research budgets, and the rapidly expanding toolbox for versatile
1043 analysis of lcWGS data now makes it an increasingly promising approach for molecular ecology,
1044 conservation and evolutionary biology research. We hope this guide will inspire broader
1045 adoption to expedite the exploration of genomic variation across the tree of life.

1046
1047
1048
1049
1050
1051
1052
1053
1054
1055
1056
1057
1058
1059
1060
1061
1062
1063
1064
1065
1066
1067
1068
1069
1070
1071
1072
1073
1074
1075

Acknowledgements

We would like to thank Philipp Messer and Robbie Davies for advice on analysis, the science Twitter community for help compiling the list of studies using lcWGS (Table S1), and Matt Hare, Matteo Fumagalli, Andy Foote, Mats Pettersson, Daniel Wegman, Jonas Meisner, Anders Albrechtsen, the Therkildsen Lab at Cornell University, and the Editor for very helpful feedback that has substantially improved this manuscript. A very special thanks to Claire Mérot for generously sharing her perspective and providing extensive suggestions that really helped make this guide more relevant, focused, and user-friendly. This study was funded through a National Science Foundation grant to NOT (OCE-1756316).

Data availability

All scripts used to generate the analysis presented in this manuscript will be available in a GitHub repository release deposited in Zenodo (DOI: 10.5281/zenodo.5037406). The NCBI SRA accession numbers for the *Heliconius* data re-analyzed in this project is available in Table S3.

Author contributions

NOT conceived of the project. All the authors designed the research jointly and collaborated to compile the overview of available methods. RNL simulated the test data and performed the comparative analysis for different experimental designs, AJ performed the analysis of the empirical data and designed the graphics, and APW performed the imputation analysis. All the authors provided input on all analyses and wrote the manuscript together.

- 1077 Aguilon, S. M., Campagna, L., Harrison, R. G., & Lovette, I. J. (2018). A flicker of hope:
1078 Genomic data distinguish Northern Flicker taxa despite low levels of divergence. *The Auk*,
1079 135(3), 748–766.
- 1080 Aguilon, S. M., Walsh, J., & Lovette, I. J. (2020). Extensive hybridization reveals multiple
1081 coloration genes underlying a complex plumage phenotype. *bioRxiv*. Retrieved from
1082 <https://www.biorxiv.org/content/10.1101/2020.07.10.197715v1.abstract>
- 1083 Alex Buerkle, C., & Gompert, Z. (2013). Population genomics based on low coverage
1084 sequencing: how low should we go? *Molecular Ecology*, 22(11), 3028–3035.
- 1085 Anderson, E. C., Skaug, H. J., & Barshis, D. J. (2014). Next-generation sequencing for
1086 molecular ecology: a caveat regarding pooled samples. *Molecular Ecology*, 23(3), 502–512.
- 1087 Andrews, K. R., Good, J. M., Miller, M. R., Luikart, G., & Hohenlohe, P. A. (2016). Harnessing
1088 the power of RADseq for ecological and evolutionary genomics. *Nature Reviews. Genetics*,
1089 17(2), 81–92.
- 1090 Auwera, G. A. V. der, & O'Connor, B. D. (2020). Genomics in the Cloud: Using Docker, GATK,
1091 and WDL in Terra. (**1st Edition**). O'Reilly Media.
- 1092 Beninde, J., Möst, M., & Meyer, A. (2020). Optimized and affordable high-throughput
1093 sequencing workflow for preserved and nonpreserved small zooplankton specimens.
1094 *Molecular Ecology Resources*. 20(6), 1632-1646
- 1095 Berner, D. (2019). Allele Frequency Difference AFD—An Intuitive Alternative to FST for
1096 Quantifying Genetic Population Differentiation. *Genes*, 10(4), 308. doi:
1097 10.3390/genes10040308
- 1098 Bilton, T. P., McEwan, J. C., Clarke, S. M., Brauning, R., van Stijn, T. C., Rowe, S. J., & Dodds,
1099 K. G. (2018). Linkage Disequilibrium Estimation in Low Coverage High-Throughput
1100 Sequencing Data. *Genetics*, 209(2), 389–400.
- 1101 Blischak, P. D., Kubatko, L. S., & Wolfe, A. D. (2018). SNP genotyping and parameter
1102 estimation in polyploids using low-coverage sequencing data. *Bioinformatics*, 34(3), 407–
1103 415.
- 1104 Bohling, J. (2020). Evaluating the effect of reference genome divergence on the analysis of
1105 empirical RADseq datasets. *Ecology and Evolution*, 10(14), 7585–7601.
- 1106 Bradburd, G. S., Coop, G. M., & Ralph, P. L. (2018). Inferring Continuous and Discrete
1107 Population Genetic Structure Across Space. *Genetics*, 210(1), 33–52.
- 1108 Browning, B. L., & Yu, Z. (2009). Simultaneous Genotype Calling and Haplotype Phasing
1109 Improves Genotype Accuracy and Reduces False-Positive Associations for Genome-wide
1110 Association Studies. *American Journal of Human Genetics*, 85(6), 847–861.
- 1111 Burgon, J. D., Vieites, D. R., Jacobs, A., Weidt, S. K., Gunter, H. M., Steinfartz, S., ... Elmer, K.
1112 R. (2020). Functional colour genes and signals of selection in colour-polymorphic
1113 salamanders. *Molecular Ecology*, 29(7), 1284–1299.
- 1114 Callahan, B. J., McMurdie, P. J., Rosen, M. J., Han, A. W., Johnson, A. J. A., & Holmes, S. P.
1115 (2016). DADA2: High-resolution sample inference from Illumina amplicon data. *Nature*
1116 *Methods*, 13(7), 581–583.
- 1117 Campagna, L., Gronau, I., Silveira, L. F., Siepel, A., & Lovette, I. J. (2015). Distinguishing noise
1118 from signal in patterns of genomic divergence in a highly polymorphic avian radiation.
1119 *Molecular Ecology*, 24(16), 4238–4251.
- 1120 Campagna, L., Repenning, M., Silveira, L. F., Fontana, C. S., Tubaro, P. L., & Lovette, I. J.
1121 (2017). Repeated divergent selection on pigmentation genes in a rapid finch radiation.
1122 *Science Advances*, 3(5), e1602404.
- 1123 Carøe, C., Gopalakrishnan, S., Vinner, L., Mak, S. S. T., Sinding, M. H. S., Samaniego, J. A., ...
1124 Gilbert, M. T. P. (2018). Single-tube library preparation for degraded DNA. *Methods in*

1125 *Ecology and Evolution / British Ecological Society*, 9(2), 410–419.

1126 Caye, K., Jumentier, B., Lepeule, J., & François, O. (2019). LFMM 2: Fast and Accurate
1127 Inference of Gene-Environment Associations in Genome-Wide Studies. *Molecular Biology*
1128 *and Evolution*, 36(4), 852–860. doi: 10.1093/molbev/msz008

1129 Cheng, J. Y., Racimo, F., & Nielsen, R. (2019). Ohana: detecting selection in multiple
1130 populations by modelling ancestral admixture components. bioRxiv doi: 10.1101/546408

1131 Chung, J. C. S., & Chen, S. L. (2017). Lacer: Accurate base quality score recalibration for
1132 improving variant calling from next-generation sequencing data in any organism. BioRxiv,
1133 130732. doi: 10.1101/130732

1134 Clucas, G. V., Kerr, L. A., Cadrin, S. X., Zemeckis, D. R., Sherwood, G. D., Goethel, D., ...
1135 Kovach, A. I. (2019). Adaptive genetic variation underlies biocomplexity of Atlantic Cod in
1136 the Gulf of Maine and on Georges Bank. *PLOS ONE*, 14(5), e0216992.

1137 Clucas, G. V., Lou, R. N., Therkildsen, N. O., & Kovach, A. I. (2019). Novel signals of adaptive
1138 genetic variation in northwestern Atlantic cod revealed by whole-genome sequencing.
1139 *Evolutionary Applications*, 12(10), 1971–1987.

1140 Davey, J. W., Hohenlohe, P. A., Etter, P. D., Boone, J. Q., Catchen, J. M., & Blaxter, M. L.
1141 (2011). Genome-wide genetic marker discovery and genotyping using next-generation
1142 sequencing. *Nature Reviews. Genetics*, 12(7), 499–510.

1143 Davies, R. W., Flint, J., Myers, S., & Mott, R. (2016). Rapid genotype imputation from sequence
1144 without reference panels. *Nature Genetics*, 48(8), 965–969.

1145 de Bakker, P. I. W., Neale, B. M., & Daly, M. J. (2010). Meta-analysis of genome-wide
1146 association studies. *Cold Spring Harbor Protocols*, 2010(6), db.top81.

1147 DeGiorgio, M., Huber, C. D., Hubisz, M. J., Hellmann, I., & Nielsen, R. (2016). SweepFinder2:
1148 increased sensitivity, robustness and flexibility. *Bioinformatics*, 32(12), 1895–1897.

1149 Domyan, E. T., Kronenberg, Z., Infante, C. R., Vickrey, A. I., Stringham, S. A., Bruders, R., ...
1150 Shapiro, M. D. (2016). Molecular shifts in limb identity underlie development of feathered
1151 feet in two domestic avian species. *eLife*, 5, e12115.

1152 Dudchenko, O., Shamim, M. S., Batra, S. S., Durand, N. C., Musial, N. T., Mostofa, R., ...
1153 Aiden, E. L. (2018). The Juicebox Assembly Tools module facilitates de novo assembly of
1154 mammalian genomes with chromosome-length scaffolds for under \$1000 bioRxiv doi:
1155 10.1101/254797

1156 Ekblom, R., & Wolf, J. B. W. (2014). A field guide to whole-genome sequencing, assembly and
1157 annotation. *Evolutionary Applications*, 7(9), 1026–1042.

1158 Excoffier, L., & Foll, M. (2011). fastsimcoal: a continuous-time coalescent simulator of genomic
1159 diversity under arbitrarily complex evolutionary scenarios. *Bioinformatics*, 27(9), 1332–
1160 1334.

1161 Felsenstein, J. (1981). Evolutionary trees from DNA sequences: a maximum likelihood
1162 approach. *Journal of Molecular Evolution*, 17(6), 368–376.

1163 Foll, M., & Gaggiotti, O. (2008). A genome-scan method to identify selected loci appropriate for
1164 both dominant and codominant markers: a Bayesian perspective. *Genetics*, 180(2), 977–
1165 993.

1166 Foll, M., Shim, H., & Jensen, J. D. (2015). WFABC: a Wright Fisher ABC-based approach for
1167 inferring effective population sizes and selection coefficients from time-sampled data.
1168 *Molecular Ecology Resources*, 15(1), 87–98.

1169 Foote, A. D., Vijay, N., Ávila-Arcos, M. C., Baird, R. W., Durban, J. W., Fumagalli, M., ... Wolf, J.
1170 B. W. (2016). Genome-culture coevolution promotes rapid divergence of killer whale
1171 ecotypes. *Nature Communications*, 7, 11693.

1172 Forester, B. R., Lasky, J. R., Wagner, H. H., & Urban, D. L. (2018). Comparing methods for
1173 detecting multilocus adaptation with multivariate genotype-environment associations.
1174 *Molecular Ecology*, 27(9), 2215–2233.

1175 Fox, E. A., Wright, A. E., Fumagalli, M., & Vieira, F. G. (2019). ngsLD: evaluating linkage

disequilibrium using genotype likelihoods. *Bioinformatics*, 35(19), 3855–3856.

Fuentes-Pardo, A. P., & Ruzzante, D. E. (2017). Whole-genome sequencing approaches for conservation biology: Advantages, limitations and practical recommendations. *Molecular Ecology*, 26(20), 5369–5406.

Fuller, Z. L., Mocellin, V. J. L., Morris, L. A., Cantin, N., Shepherd, J., Sarre, L., ... Przeworski, M. (2020). Population genetics of the coral *Acropora millepora*: Toward genomic prediction of bleaching. *Science*, 369(6501). doi: 10.1126/science.aba4674

Fumagalli, M. (2013). Assessing the effect of sequencing depth and sample size in population genetics inferences. *PLoS One*, 8(11), e79667.

Fumagalli, M., Vieira, F. G., Korneliusson, T. S., Linderöth, T., Huerta-Sánchez, E., Albrechtsen, A., & Nielsen, R. (2013). Quantifying population genetic differentiation from next-generation sequencing data. *Genetics*, 195(3), 979–992.

Fumagalli, M., Vieira, F. G., Linderöth, T., & Nielsen, R. (2014). ngsTools: methods for population genetics analyses from next-generation sequencing data. *Bioinformatics*, 30(10), 1486–1487.

Futschik, A., & Schlötterer, C. (2010). The Next Generation of Molecular Markers From Massively Parallel Sequencing of Pooled DNA Samples. *Genetics*, 186(1), 207–218.

Gaio, D., To, J., Liu, M., Monahan, L., Anantanawat, K., & Darling, A. E. (2019). Hackflex: low cost Illumina sequencing library construction for high sample counts *bioRxiv* doi: <https://doi.org/10.1101/779215>

Galinsky, K. J., Bhatia, G., Loh, P.-R., Georgiev, S., Mukherjee, S., Patterson, N. J., & Price, A. L. (2016). Fast Principal-Component Analysis Reveals Convergent Evolution of ADH1B in Europe and East Asia. *American Journal of Human Genetics*, 98(3), 456–472.

Garrison, E., & Marth, G. (2012). Haplotype-based variant detection from short-read sequencing. *bioRxiv*. Retrieved from <http://arxiv.org/abs/1207.3907>

Garrison, E., Kronenberg, Z. N., Dawson, E. T., Pedersen, B. S., & Prins, P. (2021). Vcflib and tools for processing the VCF variant call format. *bioRxiv* doi: 10.1101/2021.05.21.445151

Gatter, T., von Löhneysen, S., Drozdova, P., Hartmann, T., & Stadler, P. F. (2020). Economic Genome Assembly from Low Coverage Illumina and Nanopore Data. *bioRxiv* doi: 10.1101/2020.02.07.939454

Gautier, M. (2015). Genome-Wide Scan for Adaptive Divergence and Association with Population-Specific Covariates. *Genetics*, 201(4), 1555–1579.

Gignoux-Wolfsohn, S. A., Pinsky, M. L., Kerwin, K., Herzog, C., Hall, M., Bennett, A. B., ... Maslo, B. (2021). Genomic signatures of selection in bats surviving white-nose syndrome. *Molecular Ecology*. Retrieved from <https://onlinelibrary.wiley.com/doi/abs/10.1111/mec.15813>

Gutenkunst, R. N., Hernandez, R. D., Williamson, S. H., & Bustamante, C. D. (2009). Inferring the joint demographic history of multiple populations from multidimensional SNP frequency data. *PLoS Genetics*, 5(10), e1000695.

Haller, B. C., & Messer, P. W. (2019). SLiM 3: Forward Genetic Simulations Beyond the Wright-Fisher Model. *Molecular Biology and Evolution*, 36(3), 632–637.

Han, E., Sinsheimer, J. S., & Novembre, J. (2015). Fast and accurate site frequency spectrum estimation from low coverage sequence data. *Bioinformatics*, 31(5), 720–727.

Hayes, B. J., Visscher, P. M., McPartlan, H. C., & Goddard, M. E. (2003). Novel multilocus measure of linkage disequilibrium to estimate past effective population size. *Genome Research*, 13(4), 635–643.

Hennig, B. P., Velten, L., Racke, I., Tu, C. S., Thoms, M., Rybin, V., ... Steinmetz, L. M. (2018). Large-Scale Low-Cost NGS Library Preparation Using a Robust Tn5 Purification and Tagmentation Protocol. *G3*, 8(1), 79–89.

Huang, W., Li, L., Myers, J. R., & Marth, G. T. (2012). ART: a next-generation sequencing read simulator. *Bioinformatics*, 28(4), 593–594.

1227 Jones, F. C., Grabherr, M. G., Chan, Y. F., Russell, P., Mauceli, E., Johnson, J., ... Kingsley, D.
1228 M. (2012). The genomic basis of adaptive evolution in threespine sticklebacks. *Nature*,
1229 484(7392), 55–61.

1230 Jørsboe, E., & Albrechtsen, A. (2019). A Genotype Likelihood Framework for GWAS with Low
1231 Depth Sequencing Data from Admixed Individuals. *bioRxiv*. Retrieved from
1232 <https://www.biorxiv.org/content/10.1101/786384v1.full-text>

1233 Kim, S. Y., Lohmueller, K. E., Albrechtsen, A., Li, Y., Korneliussen, T., Tian, G., ... Nielsen, R.
1234 (2011). Estimation of allele frequency and association mapping using next-generation
1235 sequencing data. *BMC Bioinformatics*, 12, 231.

1236 Korneliussen, T. S., Albrechtsen, A., & Nielsen, R. (2014). ANGSD: Analysis of Next Generation
1237 Sequencing Data. *BMC Bioinformatics*, 15, 356.

1238 Korneliussen, T. S., & Moltke, I. (2015). NgsRelate: a software tool for estimating pairwise
1239 relatedness from next-generation sequencing data. *Bioinformatics*, 31(24), 4009–4011.

1240 Kousathanas, A., Leuenberger, C., Link, V., Sell, C., Burger, J., & Wegmann, D. (2017).
1241 Inferring Heterozygosity from Ancient and Low Coverage Genomes. *Genetics*, 205(1), 317–
1242 332.

1243 Leitwein, M., Duranton, M., Rougemont, Q., Gagnaire, P.-A., & Bernatchez, L. (2020). Using
1244 Haplotype Information for Conservation Genomics. *Trends in Ecology & Evolution*, 35(3),
1245 245–258.

1246 Li, H. (2011). A statistical framework for SNP calling, mutation discovery, association mapping
1247 and population genetical parameter estimation from sequencing data. *Bioinformatics*,
1248 27(21), 2987–2993.

1249 Li, H., & Durbin, R. (2011). Inference of human population history from individual whole-genome
1250 sequences. *Nature*, 475(7357), 493–496.

1251 Li, H., Handsaker, B., Wysoker, A., Fennell, T., Ruan, J., Homer, N., ... 1000 Genome Project
1252 Data Processing Subgroup. (2009). The Sequence Alignment/Map format and SAMtools.
1253 *Bioinformatics*, 25(16), 2078–2079.

1254 Li, H., Wu, K., Ruan, C., Pan, J., Wang, Y., & Long, H. (2019). Cost-reduction strategies in
1255 massive genomics experiments. *Marine Life Science & Technology*, 1(1), 15–21.

1256 Li, R., Li, Y., Fang, X., Yang, H., Wang, J., Kristiansen, K., & Wang, J. (2009). SNP detection for
1257 massively parallel whole-genome resequencing. *Genome Research*, 19(6), 1124–1132.
1258 doi: 10.1101/gr.088013.108

1259 Li, Y., Sidore, C., Kang, H. M., Boehnke, M., & Abecasis, G. R. (2011). Low-coverage
1260 sequencing: implications for design of complex trait association studies. *Genome*
1261 *Research*, 21(6), 940–951.

1262 Linck, E., & Battey, C. J. (2019). Minor allele frequency thresholds strongly affect population
1263 structure inference with genomic data sets. *Molecular Ecology Resources*, 19(3), 639–647.
1264 doi: 10.1111/1755-0998.12995

1265 Link, V., Kousathanas, A., Veeramah, K., Sell, C., Scheu, A., & Wegmann, D. (2017). ATLAS:
1266 Analysis Tools for Low-depth and Ancient Samples. *bioRxiv*.
1267 <https://doi.org/10.1101/105346>.

1268 Liu, S., Lorenzen, E. D., Fumagalli, M., Li, B., Harris, K., Xiong, Z., ... Wang, J. (2014).
1269 Population genomics reveal recent speciation and rapid evolutionary adaptation in polar
1270 bears. *Cell*, 157(4), 785–794.

1271 Lou, R. N., Fletcher, N. K., Wilder, A. P., Conover, D. O., Therkildsen, N. O., & Searle, J. B.
1272 (2018). Full mitochondrial genome sequences reveal new insights about post-glacial
1273 expansion and regional phylogeographic structure in the Atlantic silverside (*Menidia*
1274 *menidia*). *Marine Biology*, 165(8), 124.

1275 Lou, R. N. and Therkildsen, N. O. Batch effects in population genomic studies with low-
1276 coverage whole genome sequencing data: Causes, identification, and mitigation. *bioRxiv*.

1277 Lowry, D. B., Hoban, S., Kelley, J. L., Lotterhos, K. E., Reed, L. K., Antolin, M. F., & Storfer, A.

1278 (2017). Breaking RAD: An evaluation of the utility of restriction site-associated DNA
1279 sequencing for genome scans of adaptation. *Molecular Ecology Resources*, 17(2), 142–
1280 152.

1281 Margaryan, A., Lawson, D. J., Sikora, M., Racimo, F., Rasmussen, S., Moltke, I., ... Willerslev,
1282 E. (2020). Population genomics of the Viking world. *Nature*, 585(7825), 390–396.

1283 McCartney-Melstad, E., Mount, G. G., & Shaffer, H. B. (2016). Exon capture optimization in
1284 amphibians with large genomes. *Molecular Ecology Resources*, 16(5), 1084–1094.

1285 McKenna, A., Hanna, M., Banks, E., Sivachenko, A., Cibulskis, K., Kernytzky, A., ... DePristo,
1286 M. A. (2010). The Genome Analysis Toolkit: a MapReduce framework for analyzing next-
1287 generation DNA sequencing data. *Genome Research*, 20(9), 1297–1303.

1288 McKinney, G. J., Larson, W. A., Seeb, L. W., & Seeb, J. E. (2017). RADseq provides
1289 unprecedented insights into molecular ecology and evolutionary genetics: comment on
1290 Breaking RAD by Lowry et al. (2016). *Molecular Ecology Resources*, 17(3), 356–361.

1291 Medina, P., Thornlow, B., Nielsen, R., & Corbett-Detig, R. (2018). Estimating the Timing of
1292 Multiple Admixture Pulses During Local Ancestry Inference. *Genetics*, 210(3), 1089–1107.

1293 Meek, M. H., & Larson, W. A. (2019). The future is now: Amplicon sequencing and sequence
1294 capture usher in the conservation genomics era. *Molecular Ecology Resources*, 19(4), 795–
1295 803.

1296 Meier, J. I., Salazar, P. A., Kučka, M., Davies, R. W., Dréau, A., Aldás, I., ... Chan, Y. F. (2021).
1297 Haplotype tagging reveals parallel formation of hybrid races in two butterfly species.
1298 *Proceedings of the National Academy of Sciences of the United States of America*,
1299 118(25), 461–441.

1300 Meisner, J., & Albrechtsen, A. (2018). Inferring Population Structure and Admixture Proportions
1301 in Low-Depth NGS Data. *Genetics*, 210(2), 719–731.

1302 Meisner, J., Albrechtsen, A., & Hanghøj, K. (2021). Detecting Selection in Low-Coverage High-
1303 Throughput Sequencing Data using Principal Component Analysis *bioRxiv* doi:
1304 10.1101/2021.03.01.432540

1305 Mérot, C., Berdan, E., Cayuela, H., Djambazian, H., Ferchaud, A.-L., Laporte, M., ...
1306 Bernatchez, L. (2021). Locally adaptive inversions modulate genetic variation at different
1307 geographic scales in a seaweed fly. *Molecular Biology and Evolution*, msab143. doi:
1308 10.1093/molbev/msab143

1309 Nevado, B., Ramos-Onsins, S. E., & Perez-Enciso, M. (2014). Resequencing studies of
1310 nonmodel organisms using closely related reference genomes: optimal experimental
1311 designs and bioinformatics approaches for population genomics. *Molecular Ecology*, 23(7),
1312 1764–1779.

1313 Ni, S., & Stoneking, M. (2016). Improvement in detection of minor alleles in next generation
1314 sequencing by base quality recalibration. *BMC Genomics*, 17(1), 139. doi: 10.1186/s12864-
1315 016-2463-2

1316 Nielsen, R., Korneliussen, T., Albrechtsen, A., Li, Y., & Wang, J. (2012). SNP calling, genotype
1317 calling, and sample allele frequency estimation from New-Generation Sequencing data.
1318 *PloS One*, 7(7), e37558.

1319 Nielsen, R., Paul, J. S., Albrechtsen, A., & Song, Y. S. (2011). Genotype and SNP calling from
1320 next-generation sequencing data. *Nature Reviews. Genetics*, 12(6), 443–451.

1321 Orr, A. J. (2020). Methods for Detecting Mutations in Non-Model Organisms (Ph.D. Thesis,
1322 Arizona State University). Arizona State University, United States -- Arizona. Retrieved from
1323 <https://www.proquest.com/docview/2476130546/abstract/12747DA614FF4224PQ/1>

1324 Pasaniuc, B., Rohland, N., McLaren, P. J., Garimella, K., Zaitlen, N., Li, H., ... Price, A. L.
1325 (2012). Extremely low-coverage sequencing and imputation increases power for genome-
1326 wide association studies. *Nature Genetics*, 44(6), 631–635.

1327 Pečnerová, P., Garcia-Erill, G., Liu, X., Nursyifa, C., Waples, R. K., Santander, C. G., ...
1328 Hanghøj, K. (2021). High genetic diversity and low differentiation reflect the ecological

1329 versatility of the African leopard. *Current Biology*, 31(9), 1862-1871.e5. doi:
1330 10.1016/j.cub.2021.01.064

1331 Petkova, D., Novembre, J., & Stephens, M. (2016). Visualizing spatial population structure with
1332 estimated effective migration surfaces. *Nature Genetics*, 48(1), 94–100.

1333 Picelli, S., Björklund, A. K., Reinius, B., Sagasser, S., Winberg, G., & Sandberg, R. (2014). Tn5
1334 transposase and tagmentation procedures for massively scaled sequencing projects.
1335 *Genome Research*, 24(12), 2033–2040.

1336 Pickrell, J. K., & Pritchard, J. K. (2012). Inference of population splits and mixtures from
1337 genome-wide allele frequency data. *PLoS Genetics*, 8(11), e1002967.

1338 Powell, D. L., García-Olazábal, M., Keegan, M., Reilly, P., Du, K., Díaz-Loyo, A. P., ...
1339 Schumer, M. (2020). Natural hybridization reveals incompatible alleles that cause
1340 melanoma in swordtail fish. *Science*, 368(6492), 731–736.

1341 Pritchard, J. K., Stephens, M., & Donnelly, P. (2000). Inference of population structure using
1342 multilocus genotype data. *Genetics*, 155(2), 945–959.

1343 Puritz, J. B., & Lotterhos, K. E. (2018). Expressed exome capture sequencing: A method for
1344 cost-effective exome sequencing for all organisms. *Molecular Ecology Resources*, 18(6),
1345 1209–1222.

1346 Rastas, P. (2017). Lep-MAP3: robust linkage mapping even for low-coverage whole genome
1347 sequencing data. *Bioinformatics*, 33(23), 3726–3732.

1348 Reed, R. D., Papa, R., Martin, A., Hines, H. M., Counterman, B. A., Pardo-Díaz, C., ... McMillan,
1349 W. O. (2011). optix drives the repeated convergent evolution of butterfly wing pattern
1350 mimicry. *Science*, 333(6046), 1137–1141.

1351 Rice, E. S., & Green, R. E. (2019). New Approaches for Genome Assembly and Scaffolding.
1352 *Annual Review of Animal Biosciences*, 7, 17–40.

1353 Roesti, M., Salzburger, W., & Berner, D. (2012). Uninformative polymorphisms bias genome
1354 scans for signatures of selection. *BMC Evolutionary Biology*, 12(1), 94. doi: 10.1186/1471-
1355 2148-12-94

1356 Ros-Freixedes, R., Whalen, A., Gorjanc, G., Mileham, A. J., & Hickey, J. M. (2020). Evaluation
1357 of sequencing strategies for whole-genome imputation with hybrid peeling. *Genetics,
1358 Selection, Evolution: GSE*, 52(1), 18.

1359 Rowan, B. A., Heavens, D., Feuerborn, T. R., Tock, A. J., Henderson, I. R., & Weigel, D. (2019).
1360 An Ultra High-Density Arabidopsis thaliana Crossover Map That Refines the Influences of
1361 Structural Variation and Epigenetic Features. *Genetics*, 213(3), 771–787.

1362 Schlötterer, C., Tobler, R., Kofler, R., & Nolte, V. (2014). Sequencing pools of individuals—
1363 mining genome-wide polymorphism data without big funding. *Nature Reviews. Genetics*,
1364 15(11), 749–763.

1365 Schumer, M., Powell, D. L., & Corbett-Detig, R. (2020). Versatile simulations of admixture and
1366 accurate local ancestry inference with mixnmatch and ancestryinfer. *Molecular Ecology
1367 Resources*, 20(4), 1141–1151.

1368 Shi, S., Yuan, N., Yang, M., Du, Z., Wang, J., Sheng, X., ... Xiao, J. (2018). Comprehensive
1369 Assessment of Genotype Imputation Performance. *Human Heredity*, 83(3), 107–116.

1370 Skotte, L., Korneliussen, T. S., & Albrechtsen, A. (2012). Association testing for next-generation
1371 sequencing data using score statistics. *Genetic Epidemiology*, 36(5), 430–437.

1372 Skotte, L., Korneliussen, T. S., & Albrechtsen, A. (2013). Estimating individual admixture
1373 proportions from next generation sequencing data. *Genetics*, 195(3), 693–702.

1374 Slatkin, M. (2008). Linkage disequilibrium—understanding the evolutionary past and mapping the
1375 medical future. *Nature Reviews. Genetics*, 9(6), 477–485.

1376 Snyder-Mackler, N., Majoros, W. H., Yuan, M. L., Shaver, A. O., Gordon, J. B., Kopp, G. H., ...
1377 Tung, J. (2016). Efficient Genome-Wide Sequencing and Low-Coverage Pedigree Analysis
1378 from Noninvasively Collected Samples. *Genetics*, 203(2), 699–714.

1379 Szarmach, S., Brelsford, A., Witt, C. C., & Toews, D. (2021). Comparing divergence landscapes

1380 from reduced-representation and whole-genome re-sequencing in the yellow-rumped
1381 warbler (*Setophaga coronata*) species *bioRxiv*. Retrieved from
1382 <https://www.biorxiv.org/content/10.1101/2021.03.23.436663v1.abstract>
1383 Tang, H., Peng, J., Wang, P., & Risch, N. J. (2005). Estimation of individual admixture:
1384 analytical and study design considerations. *Genetic Epidemiology*, 28(4), 289–301.
1385 Therkildsen, N. O., & Palumbi, S. R. (2017). Practical low-coverage genomewide sequencing of
1386 hundreds of individually barcoded samples for population and evolutionary genomics in
1387 nonmodel species. *Molecular Ecology Resources*, 17(2), 194–208.
1388 Therkildsen, N. O., Wilder, A. P., Conover, D. O., Munch, S. B., Baumann, H., & Palumbi, S. R.
1389 (2019). Contrasting genomic shifts underlie parallel phenotypic evolution in response to
1390 fishing. *Science*, 365, 487–490.
1391 Tiffin, P., & Ross-Ibarra, J. (2014). Advances and limits of using population genetics to
1392 understand local adaptation. *Trends in Ecology & Evolution*, 29(12), 673–680.
1393 Turner, T. L., Hahn, M. W., & Nuzhdin, S. V. (2005). Genomic islands of speciation in
1394 *Anopheles gambiae*. *PLoS Biology*, 3(9), e285.
1395 Van Belleghem, S. M., Rastas, P., Papanicolaou, A., Martin, S. H., Arias, C. F., Supple, M.
1396 A., ... Papa, R. (2017). Complex modular architecture around a simple toolkit of wing
1397 pattern genes. *Nature Ecology & Evolution*, 1(3), 52.
1398 VanRaden, P. M., Sun, C., & O'Connell, J. R. (2015). Fast imputation using medium or low-
1399 coverage sequence data. *BMC Genetics*, 16, 82.
1400 Vieira, F. G., Albrechtsen, A., & Nielsen, R. (2016). Estimating IBD tracts from low coverage
1401 NGS data. *Bioinformatics*, 32(14), 2096–2102.
1402 Vieira, F. G., Fumagalli, M., Albrechtsen, A., & Nielsen, R. (2013). Estimating inbreeding
1403 coefficients from NGS data: Impact on genotype calling and allele frequency estimation.
1404 *Genome Research*, 23(11), 1852–1861.
1405 Vonesch, S. C., Li, S., Tu, C. S., Hennig, B. P., Dobrev, N., & Steinmetz, L. M. (2020). Fast and
1406 inexpensive whole genome sequencing library preparation from intact yeast cells *bioRxiv*
1407 doi: 10.1101/2020.09.03.280990
1408 Waples, R. S., & Do, C. (2010). Linkage disequilibrium estimates of contemporary N_e using
1409 highly variable genetic markers: a largely untapped resource for applied conservation and
1410 evolution. *Evolutionary Applications*, 3(3), 244–262.
1411 Warmuth, V. M., & Ellegren, H. (2019). Genotype-free estimation of allele frequencies reduces
1412 bias and improves demographic inference from RADSeq data. *Molecular Ecology*
1413 *Resources*, 19(3), 586–596.
1414 Westbury, M. V., Hartmann, S., Barlow, A., Wiesel, I., Leo, V., Welch, R., ... Hofreiter, M.
1415 (2018). Extended and Continuous Decline in Effective Population Size Results in Low
1416 Genomic Diversity in the World's Rarest Hyena Species, the Brown Hyena. *Molecular*
1417 *Biology and Evolution*, 35(5), 1225–1237. doi: 10.1093/molbev/msy037
1418 Wetterstrand, K. A. (2021). DNA sequencing costs: data from the NHGRI genome sequencing
1419 program (GSP) Available at www.genome.gov/sequencingcostsdata. Accessed Jan 15
1420 2021
1421 Whalen, A., Gorjanc, G., & Hickey, J. M. (2019). Parentage assignment with genotyping-by-
1422 sequencing data. *Journal of Animal Breeding and Genetics*, 136(2), 102–112.
1423 Whalen, A., Ros-Freixedes, R., Wilson, D. L., Gorjanc, G., & Hickey, J. M. (2018). Hybrid
1424 peeling for fast and accurate calling, phasing, and imputation with sequence data of any
1425 coverage in pedigrees. *Genetics, Selection, Evolution: GSE*, 50(1), 67.
1426 Whitlock, M. C., & Lotterhos, K. E. (2015). Reliable Detection of Loci Responsible for Local
1427 Adaptation: Inference of a Null Model through Trimming the Distribution of F_{ST} . *The*
1428 *American Naturalist*, 186(S1), S24–S36.
1429 Wilder, A. P., Palumbi, S. R., Conover, D. O., & Therkildsen, N. O. (2020). Footprints of local
1430 adaptation span hundreds of linked genes in the Atlantic silverside genome. *Evolution*

1431 *Letters, n/a(n/a)*. doi: 10.1002/evl3.189
1432 Zhu, Y., Bergland, A. O., González, J., & Petrov, D. A. (2012). Empirical validation of pooled
1433 whole genome population re-sequencing in *Drosophila melanogaster*. *PloS One*, 7(7),
1434 e41901.
1435 Zook, Justin M., Daniel Samarov, Jennifer McDaniel, Shurjo K. Sen, and Marc Salit. 2012.
1436 "Synthetic Spike-in Standards Improve Run-Specific Systematic Error Analysis for DNA and
1437 RNA Sequencing." *PloS One* 7 (7): e41356.
1438

1439

1440

1441 **Table 1. Total cost per sample for both library preparation and sequencing based on May**
 1442 **2021 price levels (rounded up to nearest dollar)**
 1443

Genome size (Gb)	Cost per sample (USD)*		Example organisms
	1x coverage	2x coverage	
0.2	11(3)	13(5)	Fruit fly, Honeybee, Arabidopsis
0.65	16(8)	25(17)	Atlantic silverside, Stickleback, Eastern oyster
1	21(13)	34(26)	Zebra finch, Chicken, Purple sea urchin
3	47(39)	86(78)	Human, Atlantic salmon, African clawed frog

1444
 1445 *Cost estimates do not include labor and assume that samples are sequenced efficiently on an Illumina
 1446 NovaSeq instrument. The assumed costs break down to 8 USD per library (Therkildsen & Palumbi, 2017)
 1447 and ~13 USD per Gb sequence data in a shared S4 lane (see supplementary methods for estimates of
 1448 initial investment costs). The numbers in brackets show the cost of sequencing only (i.e. the approximate
 1449 total cost with a cheap homebrew library preparation method (see section 2.2)).
 1450

Quality score recalibration		✓	✓					
Ploidy inference								HMMploidy
Genotype imputation								Beagle, LB-Impute, LinkImput, loimpute, NOISYmputer, STITCH, etc.

1454
1455
1456
1457
1458
1459
1460
1461
1462

* ngsTools is a collection of loosely-connected programs including ngsSim, ngsF, ngsPopGen, ngsUtils, ngsDist, ngs-HMM, and ngsLD

† LocalPCA can be conducted by using lostruct together with custom scripts that perform the PCA with low-coverage data (e.g. with PCAngsd).

‡ ANGSD can be used to test for statistical significance of allele frequency differentiation between two groups with the option -doAsso 1, and vcflib implements the estimation of pFst (Domyan et al. 2016)

1463
1464

Table 3. Key data filters to consider in the analysis of lcWGS data

Category	Filter	Recommendation
General filters	Base quality	Base quality scores are factored into the calculation of genotype likelihoods, so if they accurately reflect the probability of sequencing error, bases with low scores also carry useful information. However, base quality scores are sometimes miscalibrated, so noise may be reduced if bases with scores below a threshold, e.g. 20, are either trimmed off prior to analysis or ignored. Alternatively, all base quality scores can be recalibrated based on estimated error profiles in the data (see Section 3.1).
	Mapping quality	Mapping quality is not considered in genotype likelihood estimation in currently available tools, so it is often advisable to remove low-confidence and/or non-uniquely mapped reads prior to analysis (e.g. reads with mapping quality <20). Filtering out reads that do not map in proper pairs should also further increase confidence in reads being mapped to the correct location, but could cause biases in regions with structural variation.
	Minimum depth and/or number of individuals	To avoid sites with low or confounding data support in downstream analysis, minimum depth and/or minimum number of individual filters can be used to exclude sites with much reduced sequencing coverage compared to the rest of the dataset (e.g. regions with low unique mapping rates, such as repetitive sequences). Appropriate thresholds will vary between data sets, but could e.g. be to exclude sites with read data for <50% of individuals (globally or within each population), or with <0.8x average depth across individuals (after filtering on mapping quality)
	Maximum depth	Maximum depth filters are used to exclude sites with exceptionally high coverage (e.g. regions that are susceptible to dubious mapping, such as copy number variants). Common maximum depth thresholds could be one or two standard deviations above the median genome-wide depth.
	Duplicate reads	PCR and optical duplicates can give inflated impressions of how many unique molecules have been sequenced, which - particularly in the presence of preferential amplification of one allele - could bias genotype likelihood estimation. We therefore recommend removing duplicate reads prior to any analysis.

	Indels	Reads mapped to indels are frequently misaligned, especially if the ends of reads span an indel. To avoid false SNPs, we recommend either using dedicated tools to realign reads covering indels, using a haplotype-based variant caller (e.g. Freebayes or GATK) to estimate genotype likelihoods, or excluding bases flanking indels.
	Overlapping sections of paired-end reads	If the DNA insert in a library fragment is shorter than the combined length of paired reads, there will be a section of overlap between the forward and reverse reads. While some variant callers (e.g. GATK) account for the pseudo-replication in overlapping ends of read pairs, the current implementation of ANGSD treats each end of a read pair as independent (this may change in a future release (Korneliussen, personal communication)). When treated as independent, read support for overlapping sections will be “double counted”, which may bias genotype likelihoods. A conservative approach is to soft-clip one of the overlapping read ends.
Filters on polymorphic sites*	p-value	The significance threshold (often in the form of maximum p-value) can be adjusted to fine-tune the sensitivity of polymorphism detection, with lower p-values leading to fewer, but higher-confidence, SNP calls. A commonly used cut-off is 10^{-6} .
	SNPs with more than two alleles	Most software programs for downstream analyses assume that all SNPs are biallelic, so SNPs with more than two alleles can be filtered out in the SNP identification step to avoid violation of such assumptions.
	Minimum minor allele frequency (MAF)	For many types of analysis, e.g. PCA, admixture analysis, detection of F_{ST} outliers and estimation of LD, low-frequency SNPs are uninformative and can even bias results (e.g. Linck & Battey, 2019; Roesti, Salzburger, & Berner, 2012). For those types of analysis, imposing a minimum MAF filter of 1-10% can substantially speed up computation time. Appropriate thresholds depend on coverage, sample size (how many copies does a MAF threshold correspond to) and the type of downstream analysis.
Restricting analysis to a predefined site list	List of global SNPs	For comparison of parameter estimates for multiple populations, it is important to ensure that data are obtained for a shared set of sites and that SNP polarization (which allele we track the frequency of) is consistent. For programs like ANGSD where population-specific estimates are obtained by analyzing the data from each population separately, a good strategy is to first conduct a global SNP calling with all samples and then restrict population-specific analysis to those SNPs with consistent major and

		minor allele designations and no MAF or SNP p-value filter (because that would incorrectly generate “missing data” if a site is fixed in a particular population).
--	--	--

1465

1466

1467

1468

1469

1470

1471

1472

1473

1474

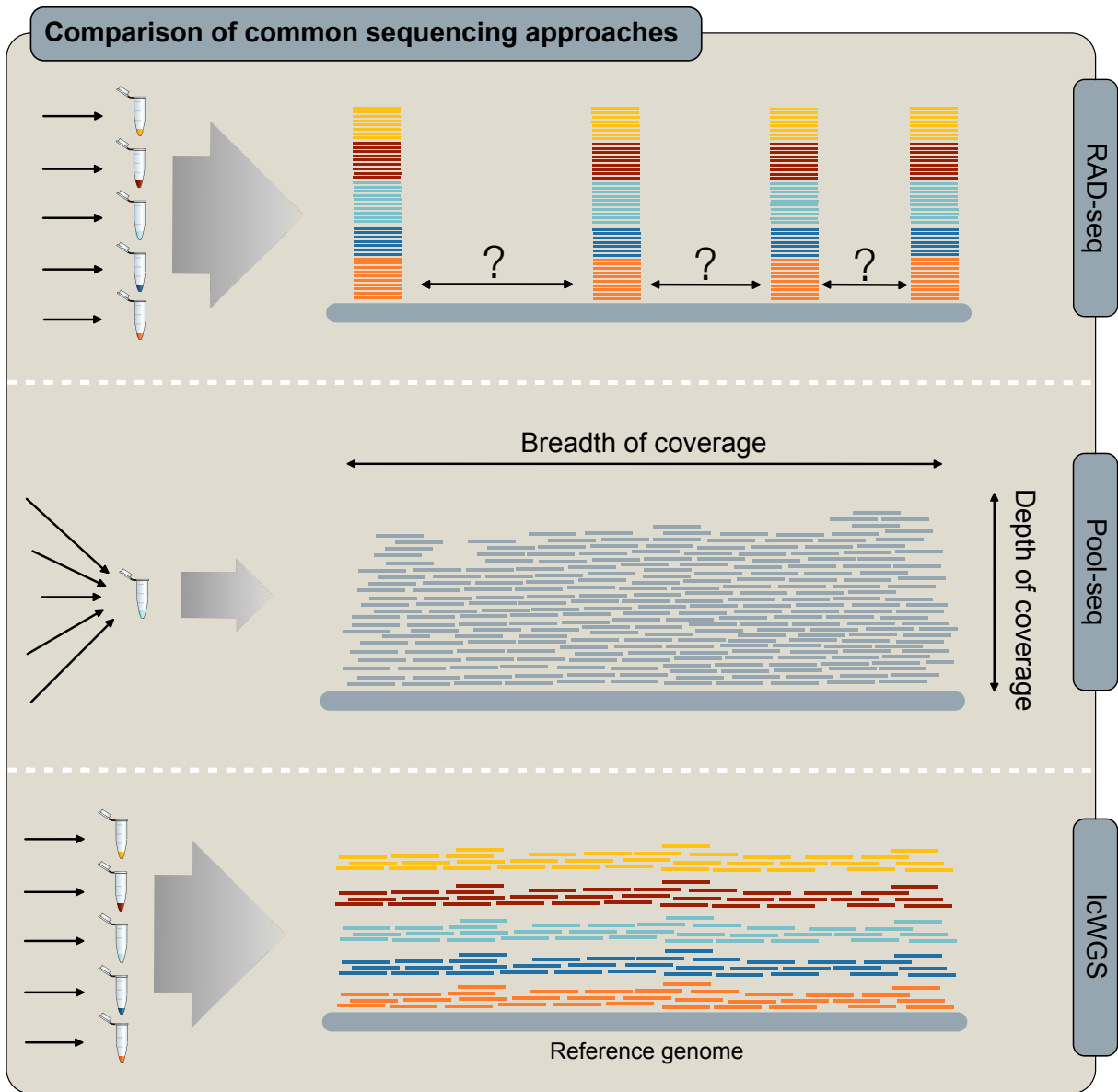
1475

* Note that no SNP significance or minimum MAF threshold should be used when estimating genetic diversity (e.g. theta and the SFS) as all sites contain relevant information. This also applies to the estimation of the absolute values of d_{xy} .

1476
1477
1478

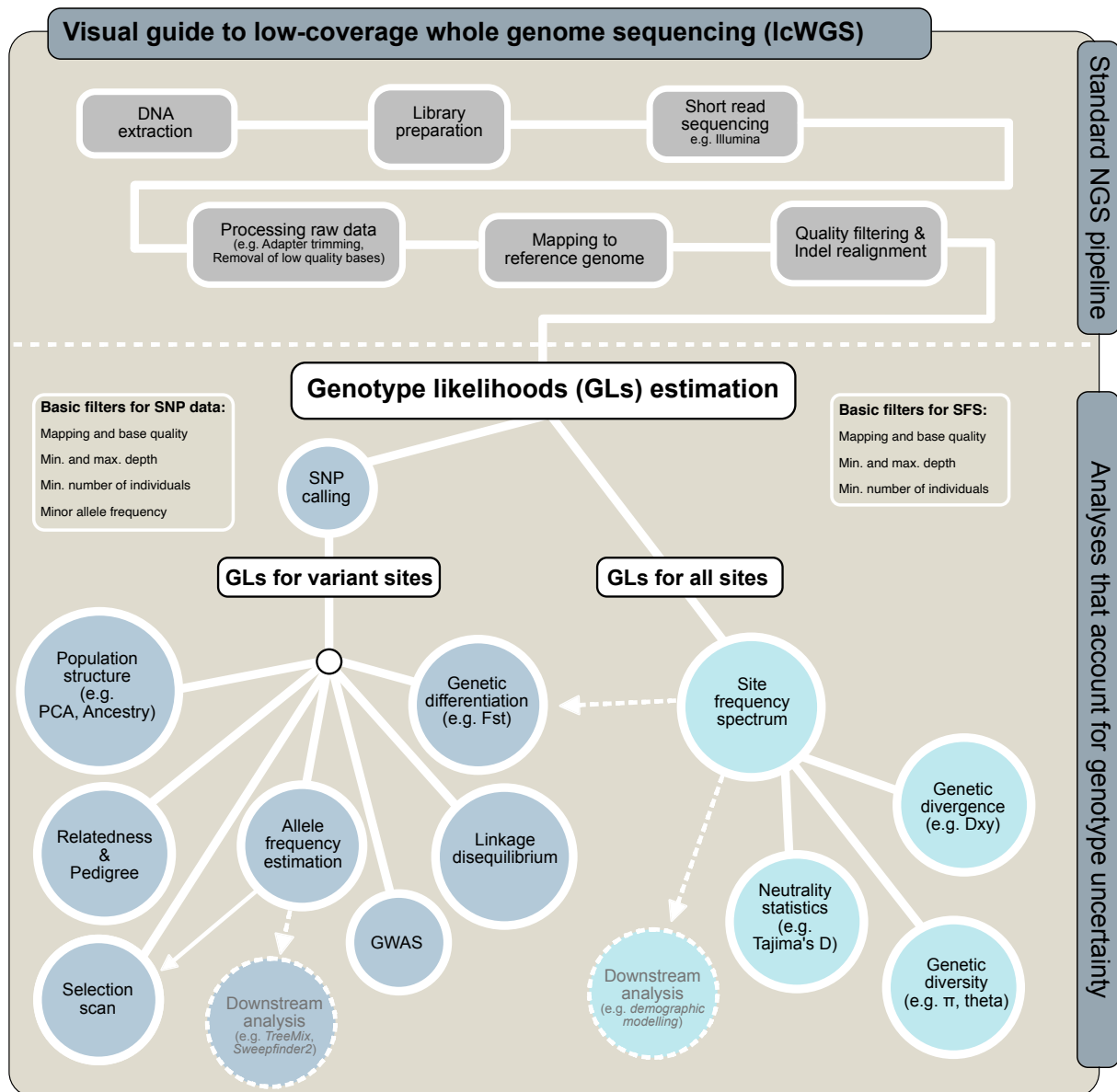
Table 4. Experimental design recommendations for different types of population genomic analyses using lcWGS data

Type of analyses	Examples	Recommendations on experimental design
Allele frequency and differentiation	Population allele frequencies, most genotype-environment association analysis (GEA) methods, F_{ST} (as implemented e.g. in vcflib), pFst	Prioritize larger sample sizes, ≥ 10 samples per population, $\geq 10x$ coverage per population, (Figure 3, 4). Avoid uneven sample size for estimation of F_{ST} (Berner, 2019)
SFS-based analyses (absolute estimation of rare-allele-dependent metrics)	Absolute estimation of Watterson's θ , Tajima's D, individual heterozygosity Reconstruction of demographic history (e.g. $\delta a \delta i$)	Prioritize higher coverage per sample, $> 4x$ coverage per sample, ≥ 5 samples per population, (Figure S2, S3).
SFS-based analyses (relative estimation of rare-allele-dependent metrics, or non-rare-allele-dependent metrics)	Relative estimation of Watterson's θ and Tajima's D (e.g. for outlier scans) π , d_{xy} , F_{ST} (as implemented in ANGSD)	Prioritize larger sample sizes, ≥ 10 samples per population, $\geq 10x$ coverage per population, (Figure 6, S2, S3, S7, S14-S17). Avoid uneven sample size for estimation of F_{ST} , (Figure S7, see also Berner, 2019).
Population structure	PCA, admixture analysis	Prioritize larger sample sizes, ≥ 10 samples per population, extremely low per-sample coverage (e.g. 0.125x, Figure 5, S6, S11) or highly uneven per-sample coverage (e.g. ranging from 0.5x to 6x, Skotte et al. 2013) can be viable.
Absolute estimation of linkage disequilibrium	LD decay rate, demographic inference	Prioritize higher coverage per sample, $\geq 4x$ coverage per sample, ≥ 20 samples per population, (Figure S4, S5; Bilton et al., 2018; Fox et al., 2019; Maruki & Lynch, 2014).
Relative estimation of linkage disequilibrium	LD pruning, LD block identification	Per-sample coverage as low as 1x could be viable, $\geq 20x$ coverage per population, (Figure S4, S5).
Genotype imputation without reference panels	STITCH, Beagle	STITCH: prioritize larger sample size (≥ 500) over per-sample coverage (1x could be sufficient), Beagle: prioritize higher per-sample coverage ($\geq 2x$) over sample sizes (≤ 250 could be sufficient), (Figure 9).



1480
 1481
 1482
 1483

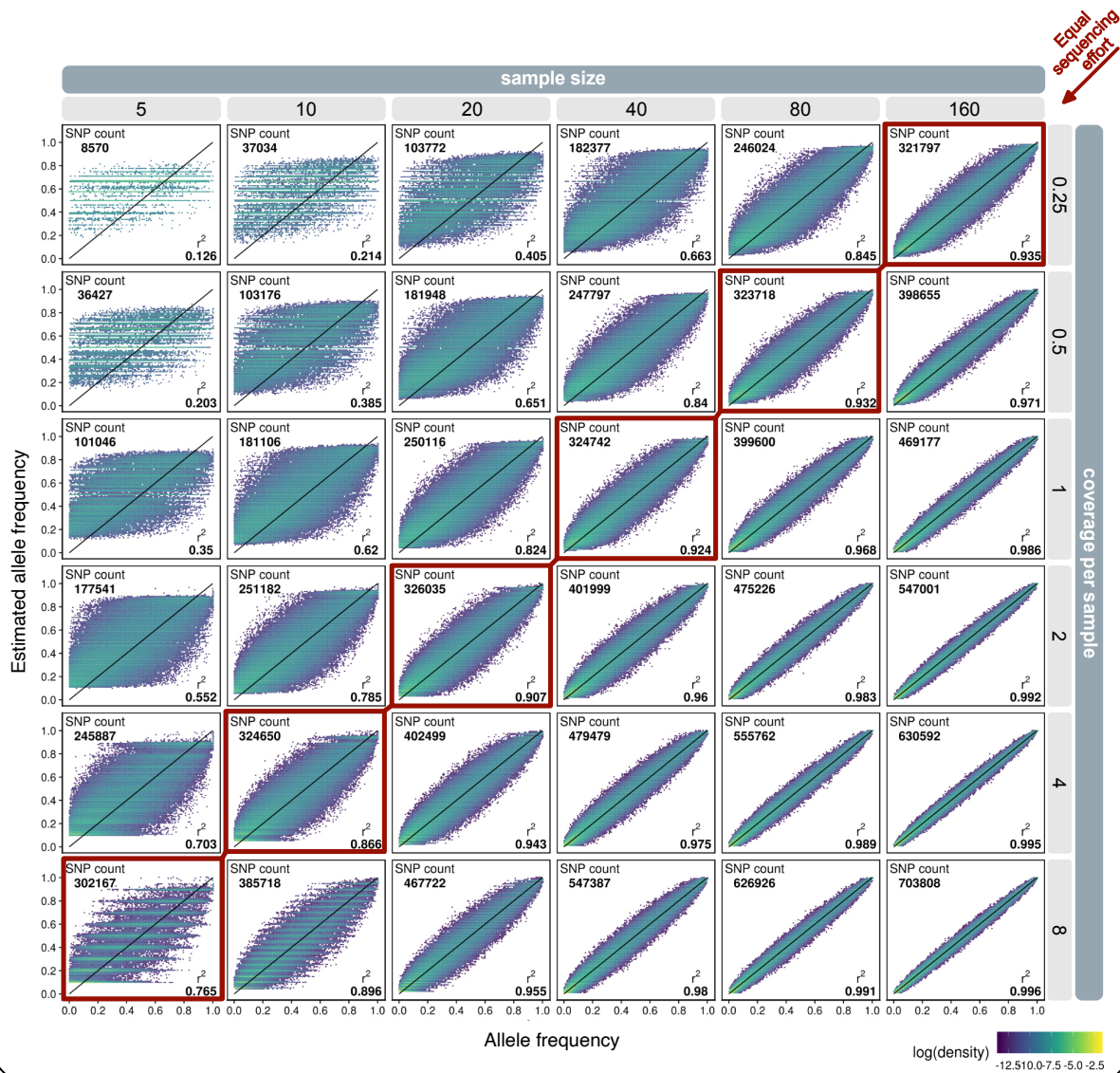
Figure 1. Diagram showing the distribution of sequencing reads mapped to a reference genome under (A) a RAD-seq, (B) a Pool-seq, and (C) a lcWGS design.



1484
 1485
 1486
 1487
 1488
 1489
 1490
 1491

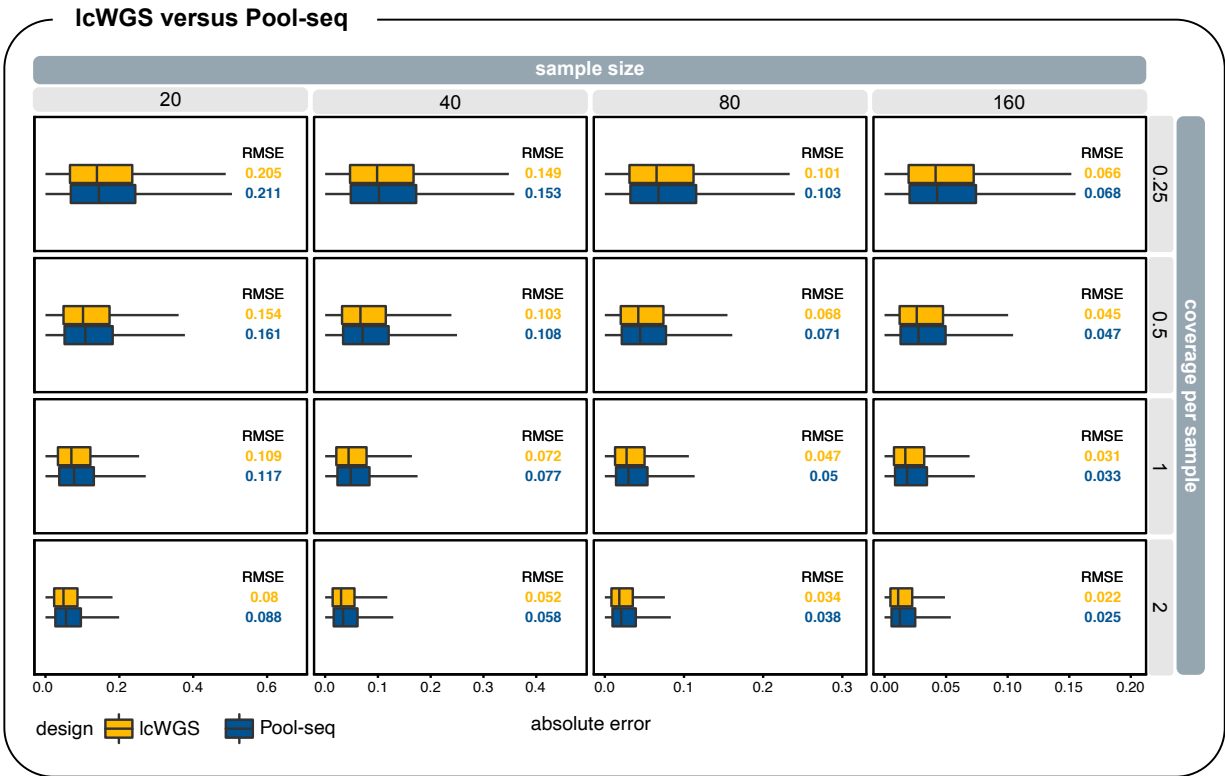
Figure 2. Diagram showing a typical computational pipeline for lcWGS data. **Top:** The data pre-processing part of the pipeline, which is similar to pipelines used for other types of NGS data. **Bottom:** The data analysis part of the pipeline, which is based on a probabilistic framework using genotype likelihoods to account for genotype uncertainty. The path through the SFS to diversity statistics and F_{ST} illustrated here reflects the workflow implemented in ANGSD. Other tools (e.g. ATLAS) can infer these statistics directly from GLs without an SFS prior.

Allele frequency estimation



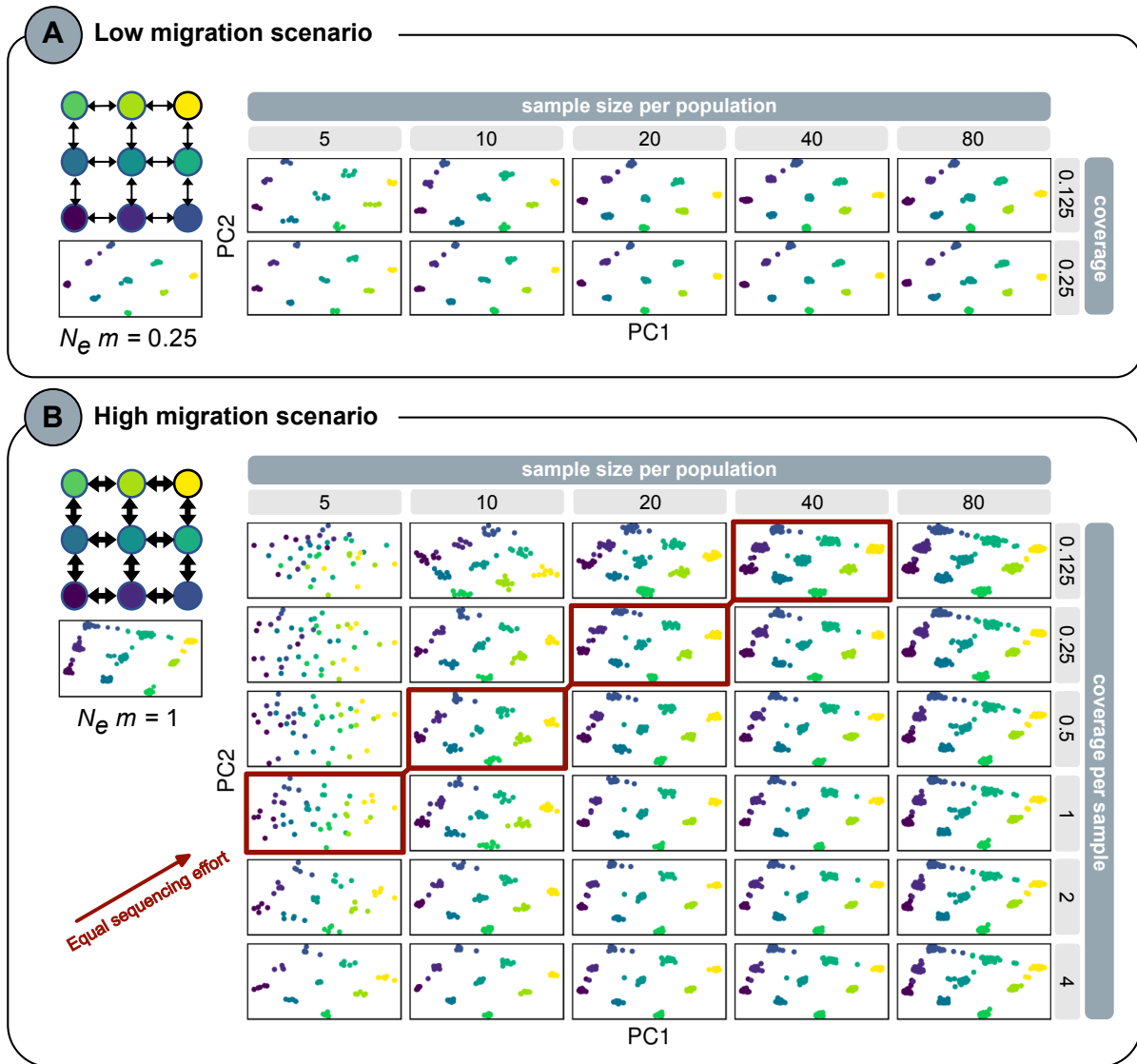
1492
1493
1494
1495
1496
1497
1498
1499
1500
1501
1502
1503

Figure 3. The estimated vs. true allele frequencies at all called SNPs (i.e. true positives + false positives) with lcWGS. Across the different facets, sample size increases from left to right, and coverage per sample increases from top to bottom. The total sequencing effort remains the same along the diagonals from bottom left to top right (one example highlighted with red boxes). The color in the plot area indicates the local density of points, with yellow corresponding to the highest density and dark blue corresponding to the lowest density. r^2 and the number of SNPs called (SNP count) are shown in each facet. The black 1:1 line in each facet indicates the positions where the estimated allele frequency is equal to the true allele frequency. False negative SNPs are not included in this figure; their distribution is shown in Figure S1.



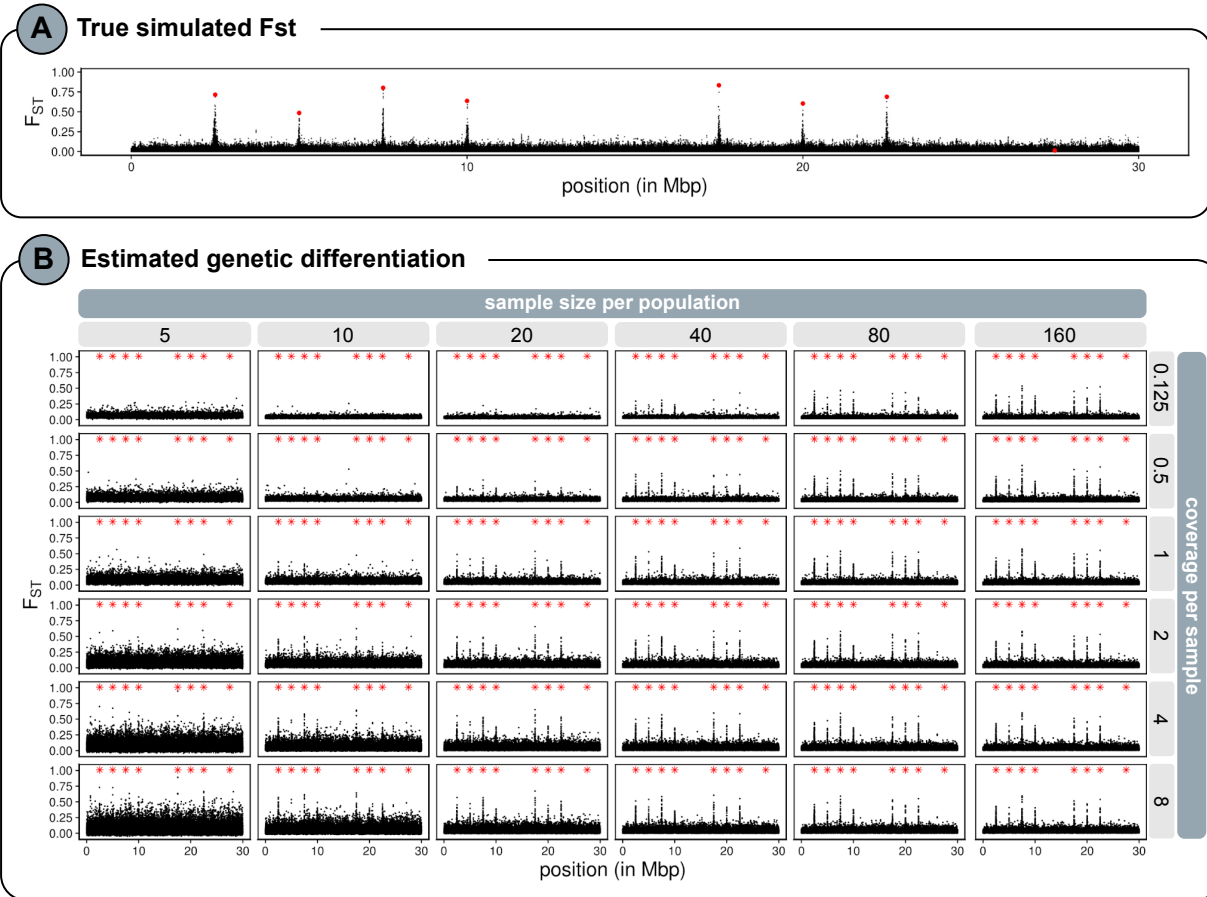
1504
 1505 **Figure 4.** A comparison of the error in allele frequency estimation with IcWGS (yellow) and
 1506 Pool-seq (blue) data. The distribution of absolute errors ($|\text{estimated frequency} - \text{true frequency}|$)
 1507 is shown with the box plots along the x-axis. The left and right hinges of the box plots show the
 1508 interquartile ranges of absolute errors, and the whiskers extend to the largest or smallest values
 1509 no further than 1.5 times the interquartile range. Outlier points are hidden. Across the different
 1510 facets, sample size increases from left to right, and coverage per sample increases from top to
 1511 bottom. The total sequencing effort remains the same along the diagonal from bottom left to top
 1512 right. The root mean squared error (RMSE) for the two sequencing designs are shown in each
 1513 facet; note the differences in scale of the x-axes. False negative SNPs are not included in this
 1514 figure; their distribution is shown in Figure S1.

1515
 1516



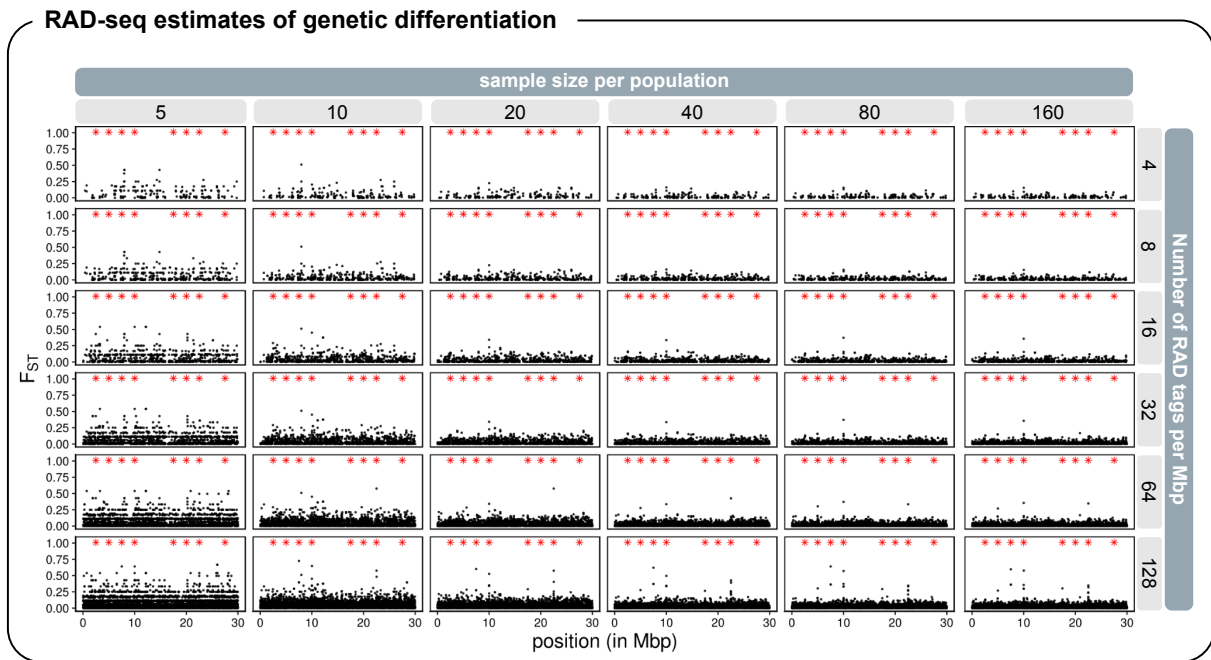
1517
 1518
 1519
 1520
 1521
 1522
 1523
 1524
 1525
 1526
 1527
 1528

Figure 5. Patterns of spatial population structure inferred through principal component analysis (PCA) with lcWGS data. **(A)** A scenario with lower gene flow (an average of 0.25 effective migrants per generation). **(B)** A scenario with higher gene flow (an average of 1 effective migrant from one population to another every generation). Left: schematics of the scenario that was simulated (each node corresponds to a simulated population) and a PCA based on the true genotypes. Right: the first two principal components from the PCA with simulated lcWGS data; each point corresponds to an individual sample and its color corresponds to the population it is sampled from. The sample size per population increases across panels from left to right, and the coverage per sample increases from top to bottom.



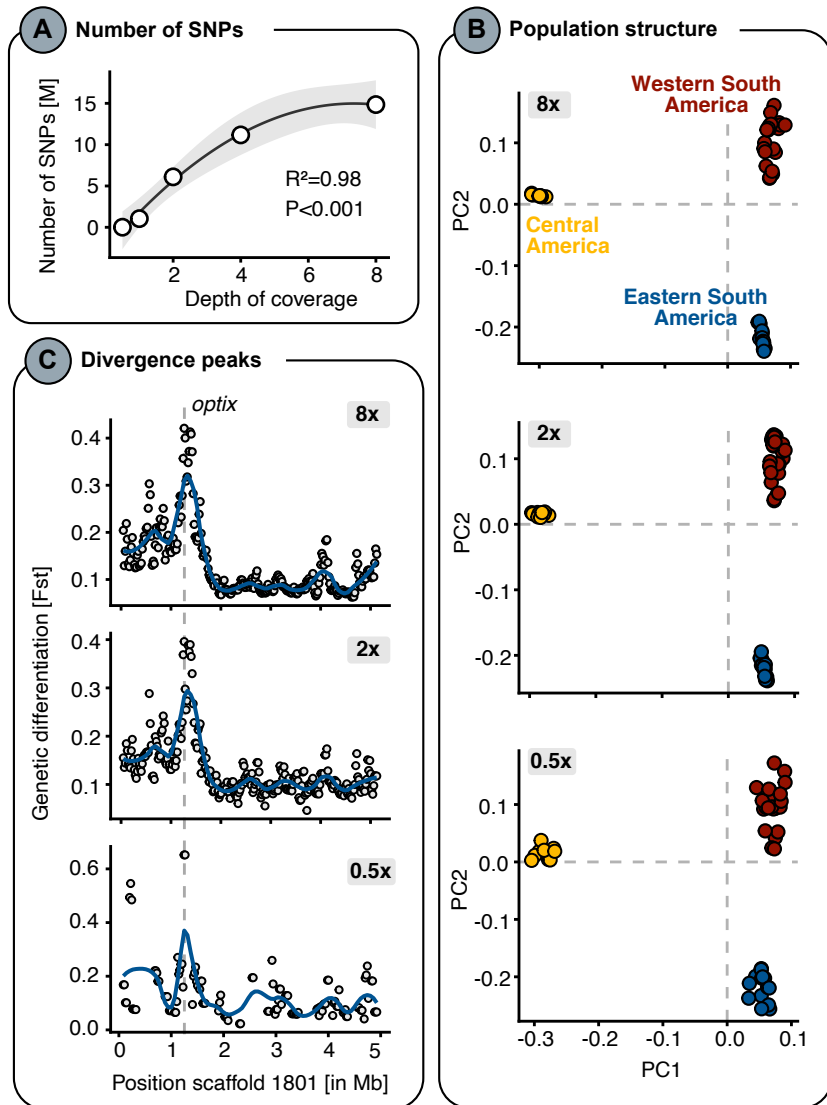
1529
 1530
 1531
 1532
 1533
 1534
 1535
 1536
 1537
 1538

Figure 6. Genome-wide scans for divergent selection with lcWGS data. **(A)** The true per-SNP F_{ST} values along the chromosome between the two simulated populations. **(B)** The F_{ST} values inferred from lcWGS data in 1kb windows along the chromosome. The sample size per population increases from left to right, and the coverage per sample increases from top to bottom. In **(A)**, the red points mark the positions of SNPs under selection and the black points mark the neutral SNPs. In **(B)**, the black points mark both the selected and neutral SNPs, and the red asterisks only mark the positions of the selected SNPs (not their inferred F_{ST} values).



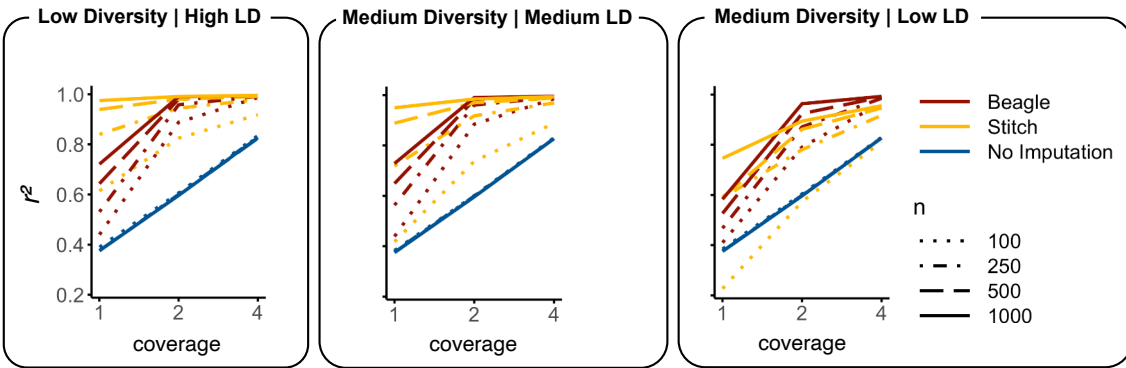
1539
 1540
 1541
 1542
 1543
 1544
 1545
 1546
 1547

Figure 7. Genome-wide scans for divergent selection with RAD-seq data. The per-SNP F_{ST} values inferred from RAD-seq data are shown on the y axis and the SNP positions are shown on the x axis. The sample size per population increases from left to right, and the RAD-tag density increases from top to bottom. The black points mark both the selected and neutral SNPs, and the red asterisks only mark the positions of the selected SNPs (not their inferred F_{ST} values).



1548
 1549 **Figure 8.** Application of genotype-likelihood-based analysis to downsampled empirical data. **(A)**
 1550 Correlation between the number of identified SNPs (in millions) and depth of sequencing
 1551 coverage in the downsampled *Heliconius* dataset. **(B)** Principal components analysis for three
 1552 different coverages (8x, 2x and 0.5x) of 51 samples. Estimates of population structure are highly
 1553 concordant across the coverage levels. Subspecies are pooled and colored by their broader
 1554 region of origin. **(C)** Estimates of genetic differentiation (F_{ST}) between *Heliconius* subspecies
 1555 with the red-bar phenotype ($n=23$) and without the red-bar phenotype ($n=28$) along the scaffold
 1556 containing the causal *optix* candidate genes in 50kb sliding windows with 20kb steps. F_{ST}
 1557 estimates are highly concordant between 8x and 2x coverage, but sparser at 0.5x due to the
 1558 lower number of identified variant sites.

1559
 1560
 1561



1562
 1563
 1564
 1565
 1566
 1567
 1568
 1569
 1570

Figure 9. Genotype imputation in STITCH and Beagle compared to posterior genotypes estimated without imputation in three simulated populations with varying diversity and linkage disequilibrium. r^2 between true genotypes and estimated genotype dosages are shown for combinations of sample size (n; with increasing n indicated by more contiguous lines), sequencing coverage (x-axis) and method (line colors).